American Mineralogist, Volume 76, pages 1061–1080, 1991

Serendibite in the Tayozhnoye deposit of the Aldan Shield, eastern Siberia, U.S.S.R.

Edward S. Grew
Department of Geological Sciences, 110 Boardman Hall, University of Maine, Orono, Maine 04469, U.S.A.
Nikolay N. Pertsev, Vladimir A. Boronikhin, Sergey Ye. Borisovskiy
Institute of the Geology of Ore Deposits, Petrology, Mineralogy, and Geochemistry of the U.S.S.R. Academy of Sciences (IGEM), Staromonetnyy per., 35 Moscow 109017, U.S.S.R.
Martin G. Yates
Department of Geological Sciences, 110 Boardman Hall, University of Maine, Orono, Maine 04469, U.S.A.
Nicholas Marquez
Aerospace Corporation, P.O. Box 92957, Los Angeles, California 90009, U.S.A.

Abstract

The Tayozhnoye iron ore deposit contains the world's most extensive development of serendibite, approximately $Ca_2(Mg,Fe^{2+})_3(Al,Fe^{3+})_{4.5}B_{1.5}Si_3O_{20}$. The Tayozhnoye serendibite is found (1) as grains, up to a few centimeters, in magnesian skarns with clinopyroxene, potassium pargasite, spinel, anorthite, uvite, phlogopite, and, locally, anhydrite and (2) as rare grains, 0.02–0.4 mm, in olivine-rich orthosilicate rock with clinohumite, K-rich pargasite, uvite, spinel, magnetite, ludwigite, and sinhalite. Based on electron and ion microprobe analyses, serendibite contains variable Fe (5.9–13.8 wt% as FeO) and relatively constant B (1.4–1.6 B atoms per formula unit). Olivine contains 1.1–1.4 wt% B_2O_3, 0.3–0.6 wt% F; clinohumite, 0.4–1.2 wt% B_2O_3, 1.0–4.3 wt% F. The sequence of mineral formation is (1) formation of skarns containing spinel [1] + anorthite + clinopyroxene and plagioclase + clinopyroxene (local orthopyroxene) during upper amphibolite to granulite-facies metamorphism (to 850 °C, 4–5 kbar); (2) introduction of B to form ludwigite, serendibite, and tourmaline (sodian uvite and uvite) at 600–700 °C; (3) replacement of earlier formed serendibite to form poikilitic uvite, calcite, spinel [2], and rare clintonite, and formation of serendibite + pargasite; and (4) low-temperature alteration to chlorite, clinozoisite, grossular, margarite, and aluminous uvite. A review of the nine localities reported worldwide for serendibite, together with T-$X(CO_2)$ and $\mu(CO_2)$-$\mu(B_2O_3)$ diagrams in the model system CaO-MgO-Al_2O_3-SiO_2-B_2O_3-CO_2-H_2O, indicate that serendibite is a mineral characteristically found in silica-undersaturated skarns metamorphosed in the presence of H_2O-rich fluids at relatively high temperatures (600–825 °C) and low to intermediate pressures (<10 kbar).

Introduction

Serendibite, a borosilicate of the aenigmatite group and approximately $Ca_2(Mg,Fe^{2+})_3(Al,Fe^{3+})_{4.5}B_{1.5}Si_3O_{20}$, has been reported from nine localities worldwide (Table 1, Appendix 1, also Deer et al., 1978). Typical associated minerals include clinopyroxene, spinel, pargasite, phlogopite (biotite), plagioclase, and calcite, but quartz is conspicuously absent. Estimated conditions of formation cover a wide range of pressures at relatively high temperatures, 1–9.5 kbar, 600–825 °C. Serendibite typically occurs in zoned metasomatic deposits (skarns) between contrasting rock types, generally marble and a feldspathic rock.

Serendibite is a rare mineral compared to other Ca-Mg-Fe-Al borosilicates, especially calcic tourmaline. The wide range of *P-T* conditions over which serendibite has formed suggests that pressure and temperature are less critical than other factors in determining the stability range of this mineral. The absence of serendibite in quartz-bearing rocks indicates that it may be restricted to certain assemblages or bulk compositions. Furthermore, serendibite is typical of metasomatic deposits. This study of the Tayozhnoye deposit, which has the most extensively developed serendibite of the nine localities listed, attempts to identify the parameters defining the stability limits of serendibite.

We believe that it is particularly appropriate to report our results on the Tayozhnoye serendibite in a volume honoring J. B. Thompson. Thompson strongly influenced the senior author's contribution to this study. In his class lectures, Thompson emphasized the importance of the composition of a given mineral in understanding its petrologic role. While Thompson concentrated on the com-

0003-004X/91/0506-1061$02.00

Table 1. World serendibite localities

Locality	Critical associated minerals*	Associated rocks**	*P, T* conditions
1. Gangapitiya, Sri Lanka	Cpx, Spl, Pl, Scp	Qtz-Fsp granulite	—
		marble	
2. Johnsburg, NY, U.S.A.	Cpx, Spl, Cal, Scp, Phl, Snh, Spr, Gdd, Tur, Prg, Kfs	Kfs rock†	6.5–8 kbar
		Dol marble	720–740 °C
3. Riverside, CA, U.S.A.	Cpx, Pl, Cal, Spl, Bt, Tur, Czo, Cln	Tonalite	1 kbar
		Dol marble	755–825 °C
4. Tayozhnoye, U.S.S.R.	Cpx, Spl, Prg, Cal, Pl, Ol, Chu, Anh, Lud, Snh, Tur, Czo, Ep, Mag, Cln, scheelite	Qtz-Fsp rocks	4–5 kbar
		Dol marbles	600–700 °C
5. Handeni district, Tanzania	Snh, Spl, Tur, Tr	In Cal marble	—
6. Melville Peninsula, NWT, Canada	Cpx, Tur, Cal, Czo, Cln, Spl	Granite	4.9–5.4 kbar
		Cal marble	700–749 °C
7. Ianapera, Madagascar	Pl, Cpx, Hbl, Zo, Czo, Tur, Grs, Crn, Spl	Serpentinite	7–9.5 kbar
		clinopyroxenite	750–800 °C
8. Ihosy, Madagascar	Pl, Scp, Cpx, Prg, Tur, Spl, Cal, Crn	Leptynite	4 kbar
		marble	700 °C
9. Russell, NY, U.S.A.	Cpx, Cal, Prg, Scp, Tur, Gdd, Phl, Spl	In calc-silicate	6.7–7.4 kbar
			660–750 °C

Note: Sources of information on serendibite localities: 1. Coomaraswamy (1902), Prior and Coomaraswamy (1903); sample BM87050. 2. Larsen and Schaller (1932); Schaller and Hildebrand (1955); Grew et al. (1991). 3. Richmond (1939); Harvard Min. Mus. sample 94852 from New City Quarry and samples Grew collected at nearby locality discovered by D.M. Morton. *P-T* conditions are those deduced by Wiechmann (1988) for metasomatism in the nearby Crestmore quarries. 4. Shabynin and Pertsev (1956); Pertsev and Nikitina (1959); Pertsev (1971); Pertsev and Boronikhin (1986, 1988); Pertsev and Kulakovsky (1987, 1988); this study. 5. von Knorring (1967); Bowden et al. (1969), sample collected by P. Bowden. 6. Hutcheon et al. (1977); Henderson (1983); U.S. Nat. Mus. sample 136851. 7 and 8. Nicollet (1988, 1990a, 1990b); C. Nicollet's samples 261g and 320. 9. Grew et al. (1990a).

* Mineral abbreviations are given in Appendix 1.

** Underlining means that serendibite-bearing skarns occur along contacts between rock types indicated.

† In addition, rare Srd in the Kfs rock itself.

mon rock-forming minerals, he also encouraged the study of the rarer ones, as these, he believed, could also lead to petrologic insight. Moreover, Thompson introduced his students to the thinking of academician D. S. Korzhinskii. Korzhinskii's students, Pertsev among them, had already worked on the Tayozhnoye deposit over 30 years ago (e.g., Shabynin and Pertsev, 1956). Thompson encouraged the senior author to carry out research in collaboration with Korzhinskii's students as part of the interacademy exchange program, which supported the senior author's research in the U.S.S.R.

Geological overview

The Tayozhnoye iron ore deposit and nearby deposits of the Leglier field are part of the Precambrian metamorphic complex of the Aldan Shield. This field is located about 550 km south of Yakutsk. Major rock units are (1) a dominantly mafic gneiss unit, largely migmatized, underlying the magnetite deposits, (2) a heterogeneous unit 300–320 m thick with magnetite deposits, and (3) an overyling gneiss unit >500 m thick (e.g., Marakushev, 1958; Pertsev, 1971; Shabynin, 1974). Unmigmatized mafic gneisses in the underlying unit are dominantly hypersthene + biotite ± clinopyroxene and clinopyroxene ± hornblende + plagioclase, locally with almandine + hypersthene and rare cordierite, whereas migmatized gneisses in the underlying unit are largely biotite granitic gneiss, injection granites, and alaskite. The middle unit consists of dolomite marble, magnesian skarns, and ultramafic orthosilicate rocks, as well as gneisses similar to those in the underlying and overlying units. Kulakovsky (1985), Kulakovsky and Pertsev (1986), and Pertsev and Kulakovsky (1988) interpreted the orthosilicate rocks, which consist largely of olivine and humite-group minerals, to be tectonically emplaced serpentinite that was subsequently metamorphosed during the high-grade events. The marbles, skarns, and ultramafic rocks are the hosts for Fe and B mineralization, largely magnetite and ludwigite, respectively. The overlying unit consists of gneisses and quartzites containing sillimanite, biotite, and, in places, cordierite; these commonly contain abundant tourmaline. The Precambrian crystalline rocks are cut by postmetamorphic Mesozoic syenite porphyries.

The Tayozhnoye deposit lies in a steeply plunging (70°) sigmoidal fold that in map pattern forms an overtipped "U" roughly 2 km × 2 km in area and opening to the southeast. The north limb of this asymmetric fold is attenuated and pinches out, while the thickened south limb can be followed to other deposits in the Leglier field. The fold developed during two periods of deformation, the second of which was associated with the main Fe mineralization. The deformation involved plastic flow of carbonate rocks and considerable faulting (Kulakovsky and Pertsev, 1986, 1987; Pertsev and Kulakovsky, 1987, 1988).

Three cycles of metamorphism are recognized, each involving a prograde and a retrograde stage (Pertsev and

Kulakovsky, 1987). Geochronologic data suggest a Proterozoic (1.9 ± 0.05 Ga) age for the most intensive event in this part of the shield. Conditions during the prograde stages of the first two cycles attained conditions of the upper-amphibolite facies and granulite facies (4–5 kbar, 650–850 °C). Granitization that produced alaskite and the most extensive development of magnesian skarns accompanied the prograde stage of the second cycle, followed by the main Fe and B mineralization at 600–700 °C during the early alkali phase of the retrograde stage. Rare andalusite formed independently of sillimanite during the retrograde stage of the first cycle. Secondary prehnite and pumpellyite could have been caused by Mesozoic hydrothermal activity accompanying the syenite porphyries (Marakushev, 1958).

B mineralization is local by comparison with Fe mineralization; ludwigite, $(Mg,Fe^{2+})_2Fe^{3+}BO_5$, is the most widespread B mineral in both the orthosilicate rocks and the dolomitic marbles. Less widespread are suanite, $Mg_2B_2O_5$, and sinhalite, $MgAlBO_4$, in the marbles and serendibite and tourmaline in magnesian skarns. The term "magnesian" refers to skarns with forsterite, clinopyroxene, or spinel ("calc-silicate" of other authors), which are distinct from the andradite + hedenbergite assemblages of calcareous skarns (e.g., Marakushev, 1958). The source of the B for ludwigite, serendibite, and tourmaline in the ore deposits and associated skarns, as well as for tourmaline in the overyling gneiss, is unknown. Possible sources include (1) a sedimentary origin for the main B mineralization in the deposit (Serdyuchenko, 1959); (2) a sedimentary origin for the tourmaline in the gneiss with metasomatic introduction into the iron ores of B remobilized from the gneisses [a possibility that Marakushev (1958) considered to be oversimplified], and (3) a metasomatic origin for all the B, introduced through hydrothermal activity associated with the alaskites and granitization (e.g., Shabynin, 1974; Pertsev and Kulakovsky, 1987). Regardless of the ultimate origin of the B, in this paper we treat the B in the serendibite-bearing rocks as having been introduced metasomatically.

Methods

The samples studied in thin section and analyzed on the electron and ion microprobes were largely obtained from drill cores; a few are from surface workings (trenches). Serendibite was found in about 15 of the approximately 400 holes drilled. About 60 thin sections of serendibite-bearing rocks were examined. Minerals were analyzed in eight thin sections (Table 2). In addition, garnet in sample 8527, which Pertsev and Boronikhin (1988, sample 1) studied in detail, and clintonite in sample 136851 (Melville Peninsula) were analyzed for comparative purposes.

Electron microprobe analyses were conducted at (1) the Institute of Geology of Ore Deposits, Petrology, Mineralogy, and Geochemistry (IGEM) of the U.S.S.R. Academy of Sciences on a Cameca MS-46 at 20 kV, 30 nA, using a full ZAF-correction method (Boronikhin and Tsepin, 1980); (2) the Institute of Geology, Yakutsk Filial, U.S.S.R. Academy of Sciences (five analyses) on Cameca Camebax-micro at 20 kV and 40 nA; and (3) the University of Maine on a MAC 400s at 15 kV and 20 nA, using Bence-Albee corrections as described by Yates and Howd (1988). Ion microprobe analyses were carried out on the Aerospace Corporation ARL ion microprobe mass analyzer. Uncertainties of 1 σ reported by Grew et al. (1990b) for this ion microprobe are ±12% of the measured value for B_2O_3, ±24% of that for Li_2O, and ±33% of that for F.

Table 2. Mineral content of the samples analyzed

	Magnesian skarns				Orthosilicate rocks			
	1	2	3	4	5	6	7	8
	5151	5152	Tzh	516		485/858*		
			255	372	2B	4A	4V	4Zh
Srd**	X	X	X	X	T†	T	T†	T
Spl	T	X	T	X	X	X	X	X
Cpx	X	X	T	X	—	—	—	—
Prg	—	T	—	—	T	T	T	X
An	—	X	—	—	—	—	—	—
Phl	—	T	X	X	T	—	T	—
Tur	X	X	T	X	T	T	T	—
Cal	T	X	X	T	—	—	—	—
Anh	—	—	—	X‡	—	—	—	—
Ol	—	—	—	—	X	X	X	X
Chu	—	—	—	—	T	X	T	T
Mag	—	X	—	T	X	X	X	X
Po			T	—	—	X	T	—
Py	T§	T§	—	X	—	—	—	—
Ccp	—	—	T	T	—	T	T	—
Ap	—	T	T	—	—	—	—	—
Zrn	—	—	T	—	T	T	—	T
Lud	—	—	—	—	T	—	T	—
Other (T)	Cln Chl	Czo Mrg Tms Ttn(?)	—	Grs Chl	Mgs	—	Snh	—

Note: X = exceeds 1% modal; T = trace.

* From sections of core no. 485 at 858.2 m and 858.4 m depth. Letters refer to individual slices of these sections.

** Mineral abbreviations are given in Appendix 1.

† Srd grains too small to analyze.

‡ Partly altered to gypsum.

§ Unidentified iron sulfide (Py or Po).

In general, the tabulated compositions combine averages of several electron microprobe analyses and one ion microprobe analysis obtained at one spot on one grain of each mineral per thin section. More spots or grains were analyzed per thin section in cases of zoning (phlogopite, tourmaline), textural variation (clinopyroxene in no. 5152), or modal variation (orthosilicate minerals, no. 458/858, 4A).

Twenty-one spots were analyzed by both the IGEM and University of Maine (UM) microprobes. In many cases, the values for the major constituents (SiO_2, Al_2O_3, FeO, MgO, CaO, K_2O) are within ±1 wt% of one another. Differences are greatest for Al_2O_3 and SiO_2, particularly for phlogopite, in which case the values of SiO_2 and Al_2O_3 obtained at IGEM are systematically higher than those obtained at UM. In other cases, the differences do

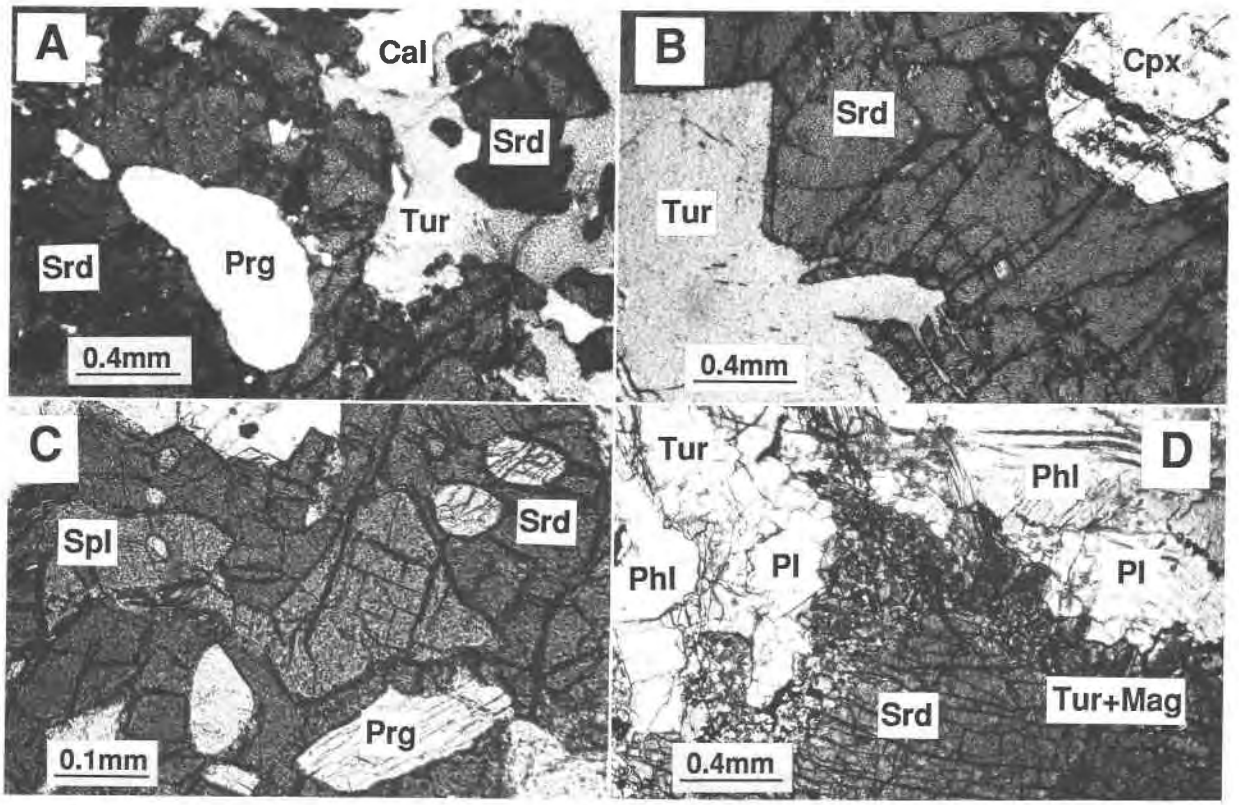

Fig. 1. Photomicrographs of magnesian skarns in plane light. (**A**) Potassium pargasite (Prg) enclosed in serendibite (Srd), which is embayed by tourmaline (Tur) containing calcite (Cal). Banding in serendibite is polysynthetic twinning. The island of serendibite is part of large grain. Sample 5152. (**B**) Aluminous (11 wt% Al_2O_3) clinopyroxene (Cpx) included in serendibite, which is embayed by tourmaline. Sample 5152. (**C**) Serendibite with inclusions of spinel (Spl, lighter gray) and pargasite. Matrix to serendibite is phlogopite and pargasite; calcite and clinopyroxene are also present in the section. Sample 3471. (**D**) Serendibite surrounded by mantle of poikilitic tourmaline with magnetite (Tur + Mag) in plagioclase (Pl) + phlogopite (Phl) matrix.

not appear to be systematic, although values of MgO obtained at IGEM tend to be lower than those obtained at UM.

Tabulated data include one analysis for each of the spots analyzed, while the discussion and figures generally consider all of the analyses.

Petrography

Two fundamentally distinct parageneses are characteristic of the Tayozhnoye serendibite: (1) magnesian skarns and (2) orthosilicate rocks, the former being by far the most widespread.

Magnesian skarns

In general, magnesian skarns include four zones developed between dolomitic marbles and an aluminosilicate rock such as biotite gneiss or granitic migmatite: (1) calcite, (2) spinel + forsterite, (3) spinel + clinopyroxene, and (4) clinopyroxene + plagioclase. Serendibite has been found only in the two zones with clinopyroxene; most commonly, it is found along the boundary between these two zones where the boundary is gradational, that is, in assemblages of clinopyroxene + spinel + calcic plagioclase (see also Shabynin and Pertsev, 1956; Pertsev and Nikitina, 1959). Serendibite is also present in magnesian skarns rich in pargasite, phlogopite, calcite, or, rarely, anhydrite. In some cases, the skarn serendibite forms irregular masses and rough crystals up to several centimeters across, nearly black in color, but blue in powder or on the rough surfaces of drill cores. In thin section, serendibite is polysynthetically twinned (Fig. 1A), is strongly pleochroic in blue, green, and yellow-brown, and shows anomalous interference colors (Pertsev and Nikitina, 1959).

Larger serendibite grains are poikilitic with inclusions of clinopyroxene (Fig. 1B), apatite, spinel (Fig. 1C), pargasite (Figs. 1A, 1C), plagioclase, phlogopite, and serendibite in grains differing in orientation from the host. Microveinlets and patches of fine-grained secondary material cut the serendibite. Serendibite is found in direct contact with clinopyroxene, plagioclase, pargasite, phlogopite, calcite, and anhydrite, although it is more com-

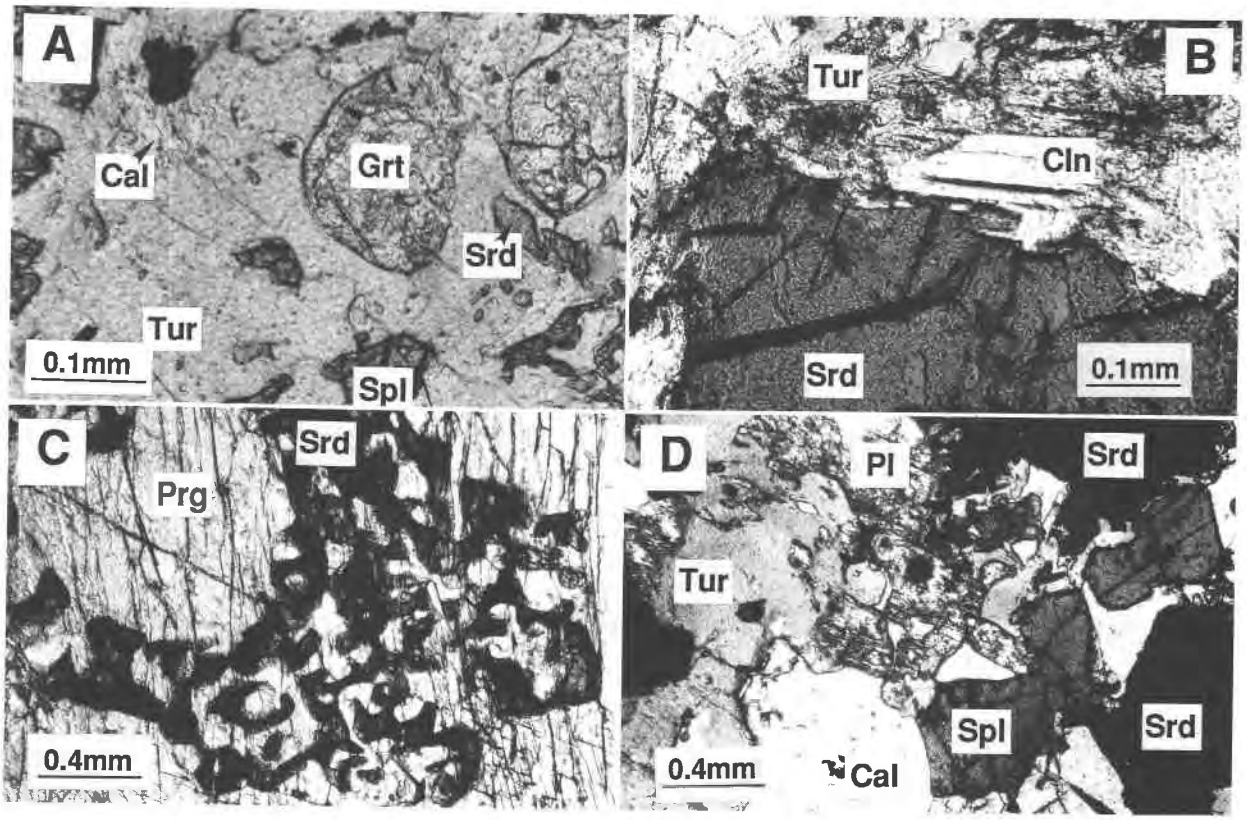

Fig. 2. Photomicrographs of magnesian skarns in plane light. (**A**) Secondary tourmaline (Tur) with inclusions of garnet (Grt), spinel (Spl), calcite (Cal), and relict serendibite (Srd). Sample 8530. (**B**) Clintonite (Cln) flake adjacent to serendibite embayed by poikilitic tourmaline. Sample 5151. (**C**) Symplectite of serendibite (dark) in pargasite (Prg). Sample 8908. (**D**) Tourmaline, calcite, spinel, and plagioclase (Pl) mostly replaced by fine-grained aggregate of clinozoisite and margarite at margin of embayed serendibite. Sample 5152.

monly overgrown by a mantle of poikilitic tourmaline (e.g., Fig. 1D).

Tourmaline is found in the zones containing clinopyroxene + plagioclase and clinopyroxene + spinel. In feldspathic rocks with biotite and either clinopyroxene, orthopyroxene, or both, in the spinel-free zone, primary tourmaline (a sodian uvite) appears instead of serendibite and forms friable aggregates of equant polygonal grains that are unzoned and dark bluish brown in the ω vibration direction. This tourmaline does not occur with serendibite. In serendibite-bearing rocks, a second variety of tourmaline forms poikilitic margins (Fig. 1D) around serendibite, in some cases, so extensively that it becomes a major constituent of the rock. This variety is typically gray-blue with a green cast, and locally zoned in color intensity, but overall is lighter in color than the primary tourmaline. Tourmaline in the margins generally has an irregular outline and embays associated minerals, but in places is euhedral against calcite. It is commonly riddled with fine inclusions, most abundantly, serendibite relics and spinel (Fig. 2A), less commonly clinopyroxene, calcite, anhydrite (sample 516/372), and magnetite. Clintonite occurs in the tourmaline mantle at its contact with serendibite in sample 5151 (Fig. 2B).

A third variety of tourmaline is deep blue, zoned, fine grained, and, locally, somewhat fibrous. This variety is found in serendibite-bearing rocks in association with clinozoisite, epidote, muscovite, margarite, and rarely chlorite.

Clinopyroxene is the dominant constituent in many of the serendibite-bearing skarns and is present in all but a few of them. Olive-green (locally brown) in hand specimen, it is nearly colorless in thin section. A few grains show anomalous interference colors. In more altered samples, clinopyroxene is turbid and riddled with fine inclusions.

Calcic plagioclase (anorthite in analyzed samples) is much less common than clinopyroxene or spinel and is replaced to a considerable extent by muscovite (in part, sericitic), margarite tufts, rare thomsonite, and clinozoisite, and in places with deep-blue tourmaline (e.g., sample 5152).

Garnet replaces plagioclase and locally forms selvages between clinopyroxene and plagioclase or pseudomorphs

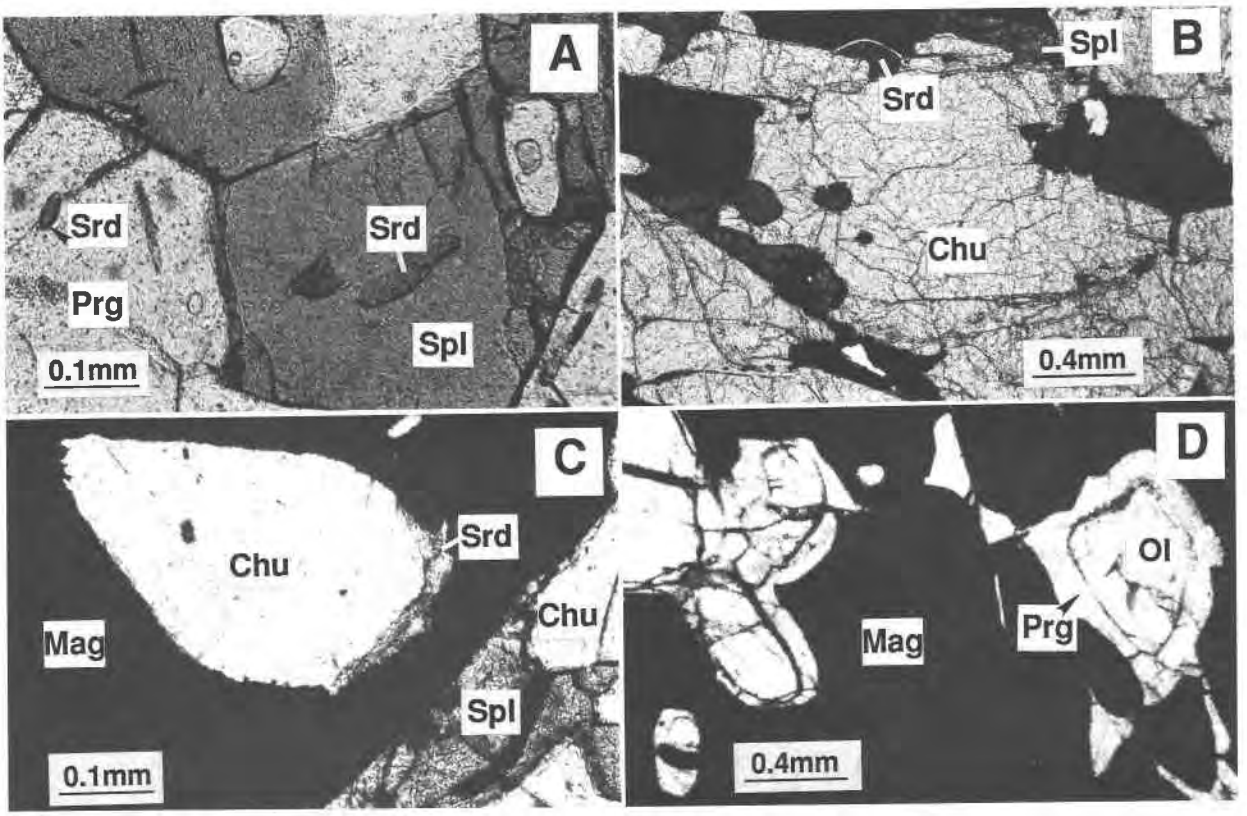

Fig. 3. Photomicrographs of a magnesian skarn (**A**) and orthosilicate rocks (**B–D**) in plane light. (**A**) Serendibite (Srd) enclosed in spinel (Spl) in pargasite (Prg). Sample 5158. (**B**) Serendibite with selvage of serpentine (?) between it and opaque (most likely magnetite) in matrix of clinohumite (Chu) with spinel. Sample 485/858, 6. (**C**) Thin margin of serendibite between magnetite (Mag) and clinohumite. Sample 485/858, 4A. (**D**) Pargasite margins around olivine (Ol, high relief) in magnetite. Sample 485/858, 4Zh.

of plagioclase. In sample 516/372, garnet and chlorite replace clinopyroxene.

Pargasite and phlogopite occur in many of the skarns and are dominant in a few. Pargasite is pale blue-gray. Phlogopite is pale brown, and in sample Tzh 255, it is zoned with brown cores and nearly colorless margins. Both minerals locally contain relics of clinopyroxene. In particular, pargasite typically penetrates and isolates clinopyroxene. In these rocks, clinopyroxene contains apparent inclusions of pargasite that may result from penetration of pargasite into clinopyroxene from outside the plane of the section. Pargasite also forms margins around spinel, isolating it from clinopyroxene. A symplectitic intergrowth with serendibite in one section (Fig. 2C) suggests coeval development of these two minerals.

Green spinel is present in almost all of the serendibite-bearing skarns. Textural relations suggest that several generations are present. Most abundant is spinel included in tourmaline formed from serendibite breakdown (Fig. 2D). In some cases, spinel is enclosed or overgrown by serendibite (Fig. 1C). Spinel overgrowths around large serendibite grains have not been found, but small serendibite inclusions are not unusual in spinel (Fig. 3A). Thus spinel developed prior to, and, in some cases, coevally with serendibite, as well as after serendibite in association with tourmaline.

Orthosilicate rocks

Serendibite was found in orthosilicate rocks from one interval 0.4 m long in a single core drill (no. 485 at a depth 858.2–858.6 m), an occurrence first described by Pertsev and Boronikhin (1986). The serendibite-bearing interval differs from other orthosilicate rocks in that olivine is more abundant than clinohumite and in that spinel and pargasite are more common. Rare relics of clinopyroxene occur in olivine associated with tourmaline at 865 m in the same drill hole (Pertsev and Boronikhin, 1986), but no clinopyroxene was found in sections containing serendibite.

Serendibite is found only in trace amounts in grains or selvages 0.02–0.4 mm across that are generally found between magnetite or spinel on the one hand, olivine or clinohumite on the other (Figs. 3B, 3C) or between magnetite and spinel. Less commonly, serendibite is included in spinel, clinohumite, or olivine. Blue-gray tourmaline appears as margins around ludwigite (locally in sample 485/858, 4V), magnetite, or spinel; it appears less commonly as isolated grains in olivine. Pargasite, also blue-

Table 3. Metamorphic history in the Tayozhnoye deposit

No.	Stage	*P, T* conditions	Minerals in magnesian skarns* and orthosilicate rocks
I	Progressive	4–5 kbar, 750–850 °C	Spl, Pl, Cpx, Opx, Ol,** Ap, Zrn, Cal
II	Retrogressive, early alkaline phase	600–700 °C	Srd, Tur(1), Lud,** Mag, Cal
III	Retrogressive, acid phase	450–600 °C	Tur(2), Prg, Phl, Cal, Anh, Srd, Snh,** Chu**
IV	Retrogressive, late alkaline phase	400 °C	Ms, Czo, Mrg, Tur(3), Chl, Grt, Srp(?),** Mgs**

Note: Adapted from Pertsev and Kulakovsky, 1987.
* Clinopyroxene + plagioclase and clinopyroxene + spinel zones only.
** Occurs only in the orthosilicate rocks. Srp(?) and Mgs are rare in the samples examined in this study.

gray in thin section, forms distinctive margins around olivine in sample 485/858, 4Zh (Fig. 3D). No reaction relationships were found among serendibite, tourmaline, and pargasite.

In sample 485/858, 4V sinhalite forms a symplectite with magnetite adjacent to ludwigite and selvages between ludwigite and magnetite.

Olivine forms subequant grains (0.5–7 mm across) in places clouded with opaque dust. In a few sections, some olivine grains have pleochroic brown patches associated with oriented acicular inclusions that are fine and abundant.

Clinohumite is locally abundant, in which case it forms inequant grains, 0.5–3 mm long, having a preferred orientation. In the other sections, clinohumite forms grains, in part pleochroic in yellow, rarely as large as 1 mm long and interstitial to the much larger olivine grains. Olivine and clinohumite are both virtually free of alteration; serpentine is rare.

Magnesite, probably a late mineral formed coevally with serpentine, occurs with tourmaline in sample 485/858, 4A.

Metamorphic history

Textures in the serendibite-bearing skarns suggest a four-stage metamorphic history (Table 3). The first stage represents original skarn formation under conditions of the upper amphibolite facies and the hornblende-granulite facies. Fe (mostly as magnetite) and B mineralization accompanied the second stage while temperatures remained high. During the third stage, fluids were introduced as temperatures decreased, resulting in the breakdown of serendibite to tourmaline, as well as the formation of additional serendibite, typically with pargasite, phlogopite, or calcite. The serendibite + pargasite assemblages suggest that the second and third stages may not be discrete, but may be the beginning and end of a continuum. Thus the anhydrous assemblage Srd + Cpx + Spl + Pl was stabilized in some rocks during introduction of the B-bearing fluids (2nd stage), whereas Srd + Prg is an intermediate assemblage, and Tur + Spl + Cal is an example of a third stage assemblage forming from serendibite (mineral abbreviations are in Appendix 1). During the fourth stage, fluids were introduced at low temperatures, resulting in the alteration of plagioclase to muscovite, clinozoisite, and margarite, and the formation of a third generation of tourmaline, the blue variety. Garnet formation and scheelite mineralization (Pertsev and Boronikhin, 1988) may belong to this stage. The orthosilicate rocks examined in this study were virtually unaffected by the fourth stage.

Thomsonite probably formed during the Mesozoic event when the syenite porphyries were emplaced.

Chemical composition

Serendibite

The Tayozhnoye serendibites contain traces of F, considerable Fe, and relatively constant B (Table 4). In formulae normalized to 14 cations and 20 O atoms, the B contents range from 1.43–1.59 atoms, close to the 1.50–

Table 4. Analyses of serendibite

	1	2	3	4	6	8
Electron microprobe analyses—wt%						
SiO_2	22.54	22.00	24.79	24.86	25.17	25.02
TiO_2	0.09	0.27	0.18	0.33	0.08	0.04
Al_2O_3	34.18	31.31	31.34	30.23	28.59	28.07
FeO	5.88	13.34	7.23	7.07	9.98	9.80
MnO	0.13	0.23	0.20	0.16	0.12	0.09
MgO	13.63	11.17	14.42	14.95	14.95	14.55
CaO	15.76	14.60	15.20	15.42	15.40	15.21
Na_2O	0.05	0.08	0	0	0.02	0
Ion microprobe analyses—wt%						
Li_2O	0.001	0.005	0.001	0.001	0.006	0.005
BeO	0	0	0.001	0	0	0.001
B_2O_3	7.80	6.77	7.54	7.06	7.04	7.42
F	0.02	0.02	0.02	0.03	0.14	0.08
SrO	—	—	0	0.001	0.001	0.001
Total	100.07	99.79	100.91	100.10	101.44	100.26
Formulae normalized to 14 cations and 20 O atoms						
Si	2.659	2.688	2.919	2.955	2.977	2.988
B	1.588	1.426	1.533	1.448	1.437	1.530
Al	1.753	1.886	1.548	1.597	1.586	1.482
Total	6.000	6.000	6.000	6.000	6.000	6.000
Ti	0.008	0.025	0.016	0.029	0.007	0.004
Al	2.999	2.622	2.802	2.638	2.399	2.469
Fe^{3+}	0.339	0.662	0.247	0.348	0.617	0.538
Fe^{2+}	0.241	0.701	0.465	0.354	0.370	0.441
Mn	0.013	0.024	0.020	0.016	0.012	0.009
Mg	2.397	2.034	2.532	2.649	2.636	2.591
Li	0	0.002	0	0	0.003	0.002
Total	5.997	6.070	6.082	6.034	6.044	6.054
Ca	1.992	1.911	1.918	1.964	1.951	1.946
Na	0.011	0.019	0	0	0.005	0
Total	2.003	1.930	1.918	1.964	1.956	1.946
F	0.008	0.008	0.006	0.012	0.053	0.029

Note: Fe measured as FeO and Fe^{3+}/Fe^{2+} is calculated from stoichiometry. Totals corrected for F = O. All electron microprobe analyses obtained at UM.

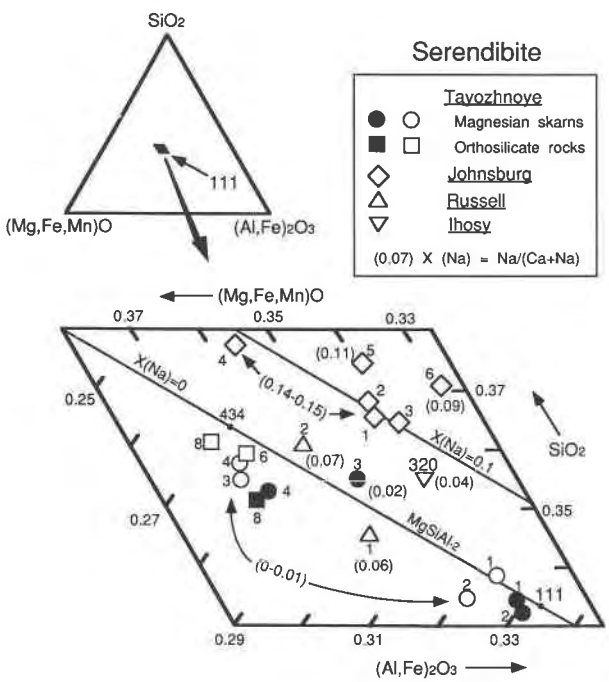

Fig. 4. Composition of serendibite in terms of molecular proportions of (Mg,Fe,Mn)O, $(Al,Fe)_2O_3$, and SiO_2. Tayozhnoye compositions normalized to 20 O atoms, 14 cations to estimate Fe^{3+} and Fe^{2+} contents, whereas Fe is assumed to be FeO in the Fe-poor Johnsburg, Russell, and Ihosy compositions. For Tayozhnoye, unfilled symbols refer to UM analyses, filled symbols refer to IGEM analyses, numbers refer to samples in Table 2. For Johnsburg, numbers correspond to samples as follows: 1 = Sl-3 core, 2 = Sl-3 rim, 3 = 5231, 4 = 18964, 5 = Sl-4, and 6 = 84-5 (Grew et al., 1991). For Russell, 1 and 2 refer to two grains in the analyzed section (Grew et al., 1990a). For Ihosy, 320 = sample 320 (Nicollet, 1988, 1990b). Spacing between Tschermak substitution lines calculated from $NaSiCa_{-1}Al_{-1}$. The numbers in parentheses with arrows are ranges of X(Na) for Tayozhnoye (except sample 3, IGEM) and for Johnsburg samples 1–4. Dots marked 111 and 434 indicate ratios of (Mg,Fe,Mn)O, $(Al,Fe)_2O_3$, and SiO_2.

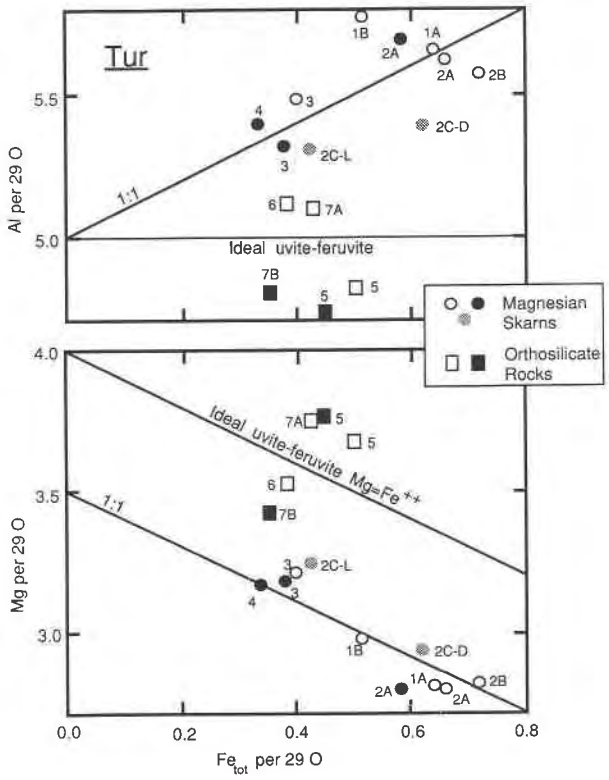

Fig. 5. Compositions of Tayozhnoye uvite in terms of Fe_{tot}, Mg, and Al atoms per 29 O atoms (ideal formulation of three B atoms and four OH^-). Lines indicating 1:1 substitution are for reference only. Numbers refer to samples in Table 2, letters to individual grains, where 2C-L and 2C-D refer to lighter and darker zones in grain C of sample 5152. Unfilled symbols = UM analyses, filled symbols = IGEM analyses, stippled symbols = Institute of Geology, Yakutsk, analyses. Ideal uvite-feruvite solid solution is $Ca(Mg,Fe^{2+})_3MgAl_5Si_6B_3O_{27}(OH)_4$.

1.54 atoms measured for Johnsburg serendibite by Grew et al. (1991). In addition, the B contents of 1.59 and 1.43 atoms in samples 5151 and 5152 (nos. 1 and 2) measured with the ion microprobe agree with the 1.61 and 1.46 B atoms obtained in crystal structural refinements of serendibite in these samples (P. K. Sen Gupta and G. H. Swihart, unpublished data; see also Sen Gupta et al., 1989). Calculated Fe^{3+} contents are 35–63% of the total Fe. The dominant compositional variation in the Tayozhnoye serendibite is related to a Tschermak-type substitution: $(Mg,Fe^{2+})Si(Al,Fe^{3+})_{-2}$ (Fig. 4). Tayozhnoye serendibite compositions plot in an elongated area oriented parallel to one for the Johnsburg serendibite compositions, but displaced to lower SiO_2. This displacement is approximately that calculated for 10% substitution of Ca by Na from the exchange $NaSiCa_{-1}Al_{-1}$, which is also characteristic of aenigmatite (Deer et al., 1978). Discrepancies between the plotted serendibite compositions and positions estimated from $NaSiCa_{-1}Al_{-1}$ probably arise as much from uncertainty in the estimated ratio of Fe^{3+}/Fe^{2+} as from analytical errors.

Tourmaline

The blue-gray tourmaline in serendibite-bearing skarns and orthosilicate rocks is uvite with X_{Ca} = Ca/(Ca + Na) = 0.89–1.0 (Table 5). Uvite from the magnesian skarns deviates from the ideal formula for uvite-feruvite solid solution, $Ca(Mg,Fe^{2+})_3MgAl_5Si_6B_3O_{27}(OH,F)_4$ (Dunn et al., 1977; Grice and Robinson, 1989) in that Mg + Fe = 3.5 and Al increases from 5.3 to 5.8 with increasing Fe (Fig. 5). On the other hand, uvite from the orthosilicate rocks has (Mg + Fe) and Al contents closer to the values of 4 and 5 in the ideal uvite formula. Association with magnetite and Fe^{3+}-bearing serendibite suggests that a substantial proportion of the Fe in the uvite is ferric. Inasmuch as the uvite compositions plot close to or above the uvite-feruvite join in Figure 6, we infer that Fe^{3+} substitutes for Mg on the Y site rather than for Al on the Z site [site notation $XY_3Z_6Si_6B_3O_{27}(OH)_4$, Deer et al., 1986].

Table 5. Analyses of tourmaline

	1* UM	2* UM	2** UM	3* UM	4* IGEM	5* UM	6* UM	7* UM
				Electron microprobe analyses—wt%				
SiO_2	35.40	35.87	31.93	35.72	36.41	37.20	36.34	35.90
TiO_2	0.05	0.05	0.02	0.35	0.43	0.09	0.06	0
Al_2O_3	29.30	29.33	38.59	28.69	28.10	25.24	26.48	26.64
FeO	4.67	4.83	6.89	2.94	2.45	3.68	2.79	3.14
MnO	0	0.01	0.04	0.01	0	0	0.00	0.05
MgO	11.53	11.54	5.39	13.29	13.07	15.21	14.43	15.45
CaO	5.28	4.97	2.95	5.29	5.22	5.69	5.69	5.57
Na_2O	0.17	0.25	1.28	0.25	0.08	0.14	0.03	0.08
K_2O	0.01	0.02	0	0	0	0	0.04	0.06
				Ion microprobe analyses—wt%				
Li_2O	0	0.001	0.001	0	0	0.002	0	0.001
B_2O_3	9.90	9.79	11.24	9.72	10.02	11.81	9.69	11.15
SrO	0.007	0.003	0.02	0.04	0.03	0.007†	0.009	0.02†
BaO	0	0	0	0	—	—	—	—
F	0.27	0.32	0.01	0.70	0.75	1.32	0.59	1.56
				Calculated—wt%				
H_2O	3.50	3.48	3.71	3.31	3.29	3.13	3.33	2.97
Total	99.98	100.33	102.07	100.02	99.53	102.96	99.23	101.93
				Formulae for 29 O atoms				
Si	5.858	5.915	5.160	5.883	5.989	5.936	6.033	5.798
B	2.828	2.787	3.134	2.763	2.845	3.253	2.777	3.108
Ti	0.006	0.006	0.002	0.043	0.053	0.011	0.007	0
Al	5.715	5.701	7.350	5.569	5.447	4.747	5.181	5.071
Fe	0.646	0.666	0.931	0.405	0.337	0.491	0.387	0.424
Mn	0	0.001	0.005	0.001	0	0	0	0.007
Mg	2.845	2.837	1.299	3.263	3.205	3.618	3.571	3.720
Li	0	0.001	0.001	0	0	0.001	0	0
Ca	0.936	0.878	0.511	0.934	0.920	0.973	1.012	0.964
Na	0.055	0.080	0.401	0.080	0.026	0.043	0.010	0.025
K	0.002	0.004	0	0	0	0	0.008	0.012
Sr	0.001	0	0.001	0.004	0.003	0.001	0.001	0.002
Total	18.892	18.876	18.795	18.945	18.825	19.074	18.987	19.131
F	0.141	0.167	0.005	0.365	0.390	0.666	0.310	0.797
OH	3.859	3.833	3.995	3.635	3.610	3.334	3.690	3.203

Note: All Fe as FeO; (OH + F) assumed to equal 4. Totals corrected for F = O. UM and IGEM indicate the electron microprobe used.
* Blue-gray uvite.
** Blue, aluminous uvite. Ion microprobe values are averages of two spots.
† Also 0.001 wt% Rb_2O.

This substitution is consistent with the inverse relation between Mg and Fe in uvite from the skarns (Fig. 5). Because the ratio of Fe^{3+}/Fe^{2+} has not been determined, inferring a substitution scheme for Mg, Fe, and Al is not possible.

Zoning in the uvite appears to be related to Ti and Fe contents, which were found in one case to be higher in a darker zone (TiO_2 = 0.51 wt%, Fe as FeO = 4.53 wt%) than in the adjacent lighter-colored zone (TiO_2 = 0.33 wt%, Fe as FeO = 3.14 wt%) (Figs. 5 and 6).

Blue tourmaline is an aluminous uvite with $X(Ca)$ = 0.54–0.56 and differs markedly from the earlier formed uvite in the same sample (no. 2) in its higher Al (Fig. 6) and lower Si and F contents (Table 5). Because Li contents are negligible in the aluminous uvite, the extra Al appears to be incorporated by a Tschermak substitution, $^{[7]}Al + {}^{[4]}Al = {}^{[7]}(Mg,Fe) + {}^{[4]}Si$ (Henry and Guidotti, 1985).

B_2O_3 contents determined with the ion microprobe are 9.69–11.81 wt%, that is, within the expected analytical uncertainty of ±1.5 wt% (Grew et al., 1990b) of the corresponding ideal B_2O_3 contents of 10.3–10.9 wt% (for three B atoms per formula unit).

Clinopyroxene and clinoamphibole

Clinopyroxene is aluminous diopside with close to one Ca atom per formula unit (Table 6). In sample 5152 (no. 2), it is heterogeneous: the difference between $^{[4]}Al$ and $^{[6]}Al$ (corrected for Ti) and Fe_{tot} increase with Al_{tot}, a relation suggesting incorporation of Fe through the substitution $^{[6]}Fe^{3+}\,{}^{[4]}AlMg_{-1}Si_{-1}$.

The clinoamphiboles are pargasite and potassium pargasite with $X_K = K/(K + Na)$ = 0.42–0.63 in the orthosilicate rocks and X_K = 0.62–0.74 in sample 5152 (no. 2), a skarn (Table 7; Fig. 1A). This potassium pargasite also contains 0.39–0.57 wt% Cl (IGEM probe). Pargasite X_K increases with increasing X_{Fe} [= $Fe_{tot}/(Fe_{tot}$ + Mg)] and with decreasing $^{[4]}Al$ (Fig. 7), trends reported in other K-rich amphibole samples from silica-undersaturated skarns (Shimazaki et al., 1984; Matsubara and Motoyoshi, 1985).

Phlogopite, clintonite, margarite, and chlorite

Phlogopite is relatively Ti poor and Si rich; zoning in coarse flakes in sample Tzh 255 (no. 3) is correlated with Ti and Fe, with darker cores slightly richer in these constituents than lighter margins (Table 8).

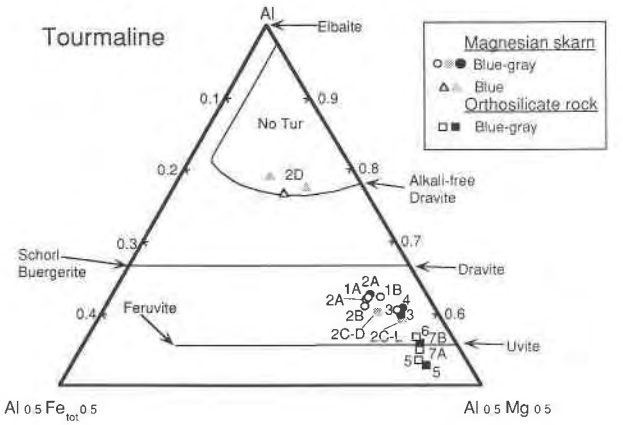

Fig. 6. Al-Fe_{tot}-Mg diagram (in atomic proportions) for uvite from the Tayozhnoye deposit (adapted from Henry and Guidotti, 1985). The triangles 2D refer to the blue aluminous uvite associated with margarite and clinozoisite in sample 5152 (no. 2). Otherwise, symbols are the same as in Figure 5. None of the 393 tourmaline compositions compiled by Henry and Guidotti (1985) plot in the field marked here as No Tur.

TABLE 6. Analyses of clinopyroxene

	1 UM	2* UM	2** UM	3 IGEM	4 IGEM
	Electron microprobe analyses—wt%				
SiO_2	51.01	44.57	51.45	51.09	48.98
TiO_2	0.25	0.86	0.49	0.38	0.72
Al_2O_3	4.78	10.95	3.59	5.61	5.67
FeO	2.55	6.85	3.50	3.03	2.82
MnO	0.19	0.22	0.12	0.18	0.10
MgO	16.23	11.56	15.82	15.35	15.24
CaO	25.20	24.57	24.56	24.53	24.43
Na_2O	0.12	0.10	0.17	0.30	0
	Ion microprobe analyses—wt%				
Li_2O	—	0.002	—	—	—
B_2O_3	—	0.096	—	—	—
SrO	—	0.005	—	—	—
F	—	0.009	—	—	—
Total	100.33	99.79	99.70	100.51†	98.96
	Formulae normalized to 6 O atoms				
Si	1.861	1.675	1.893	1.860	1.820
Al	0.139	0.319	0.107	0.140	0.180
B	—	0.006	—	—	—
Total	2.000	2.000	2.0	2.0	2.0
Ti	0.007	0.024	0.014	0.010	0.020
Al	0.067	0.166	0.049	0.101	0.068
Fe	0.078	0.215	0.108	0.092	0.088
Mn	0.006	0.007	0.004	0.006	0.003
Mg	0.883	0.648	0.868	0.833	0.844
Total	1.041	1.060	1.043	1.042	1.023
Ca	0.985	0.990	0.968	0.957	1.012
Na	0.008	0.007	0.012	0.021	0
Total	0.993	0.997	0.980	0.978	1.012
Total cat.	4.034	4.057	4.023	4.020	4.035
F	—	0.001	—	—	—

Note: All Fe as FeO. UM and IGEM indicate the electron microprobe used.
* Enclosed in serendibite.
** In matrix to serendibite.
† Total includes 0.04 wt% K_2O.

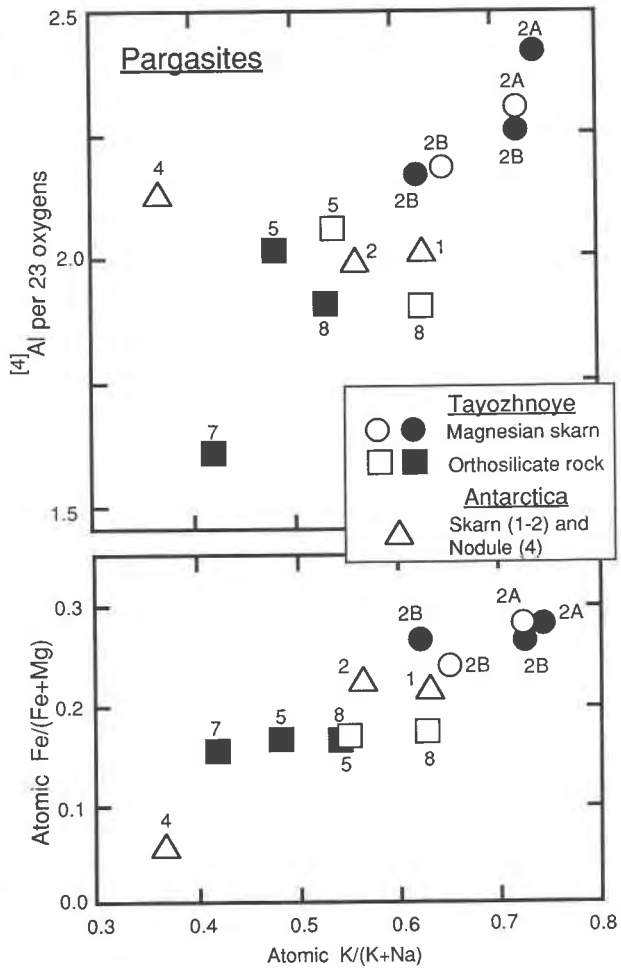

Fig. 7. Compositions of pargasite and potassium pargasite in terms of the atomic ratio of Fe/(Fe + Mg) (Fe_{tot}), $^{[4]}Al$ (calculated as 8 − Si and ignoring B) and the atomic ratio of K/(K + Na_{tot}). Sources of data: (1) Magnesian skarn and orthosilicate rock, this study, numbers refer to samples listed in Table 2, letters refer to individual grains, of which 2B was analyzed at two different spots at IGEM; unfilled symbols = UM data, filled symbols = IGEM data. (2) Skarn and nodule, from Matsubara and Motoyoshi (1985), numbers refer to analyses listed in their Table 1.

Clintonite formed from serendibite breakdown in sample 5151 (no. 1) (Tayozhnoye) and in sample 136851 (Melville Peninsula) are similar compositionally, except in F content (Table 8), and are low in Si (Si = 2.31–2.39) and intermediate in Fe_{tot} (Fe = 0.20–0.28) compared to clintonite overall (Si = 2.22–2.72, Fe^{2+} + Fe^{3+} ≤ 0.66 per 22 O atoms, Guggenheim, 1984).

Margarite is close to the end-member in composition except for 4 mol% paragonite solid solution (Table 8).

Chlorite closely associated with garnet in sample 516/372 (no. 4) is less magnesian than phlogopite in the same thin section (Table 8). This Fe-Mg fractionation is the reverse of that for most biotite + chlorite pairs (e.g., Al-

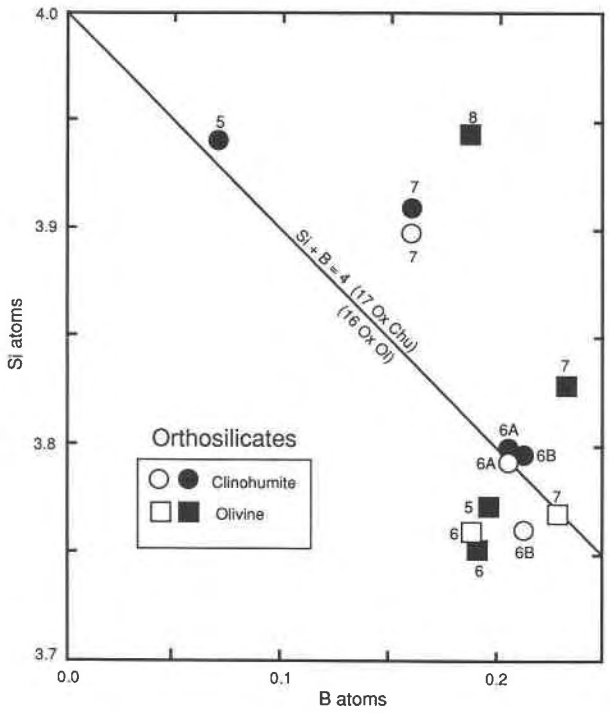

Fig. 8. B and Si contents of olivine and clinohumite in terms of ideal formulations: $4Mg_2SiO_4$ and $Mg_9Si_4O_{16}(OH)_2$. Unfilled symbols = UM data, filled symbols = IGEM data, numbers refer to samples in Table 2, letters to individual grains.

bee, 1968) and implies that the late-formed chlorite did not equilibrate with phlogopite.

Olivine and clinohumite

Olivine (X_{Fe} = 0.11–0.15) is unique in its high B_2O_3 (1.1–1.4 wt%) and F (0.33–0.60 wt%) contents (Table 9), constituents rarely sought in olivine and then generally detected only at the trace level (e.g., Steele et al., 1981; Kohn et al., 1989), even in association with kornerupine (Grew, 1988). Clinohumite (X_{Fe} = 0.08–0.11) contains 0.37–1.2 wt% B_2O_3, matching the maximum reported in a humite-group mineral (chondrodite, Hinthorne and Ribbe, 1974). In formulae normalized to 16 and 17 O atoms, respectively, B + Si is approximately equal to 4 for both olivine and clinohumite (Fig. 8). An inverse relation of B and Si is reported in some minerals with a variable B content, such as chondrodite (Hinthorne and Ribbe, 1974) and sillimanite (Grew and Hinthorne, 1983), but to date only in kornerupine has extensive B-Si miscibility been demonstrated for a single tetrahedral site (e.g., Moore and Araki, 1979).

D. R. Veblen (personal communication, 1990) has examined homogeneous patches of olivine with the transmitting electron microscope and found no B-rich inclusions. Thus B is incorporated in the olivine itself. Pending further study by Veblen, which is now in progress, inferring a substitutional scheme for B incorporation is premature. Because the Al_2O_3 contents of the olivine are below the detection limit of the electron microprobe at UM (i.e., less than 0.1 wt% Al_2O_3), solid solution of sinhalite, $(Mg,Fe)AlBO_4$, a mineral isostructural with olivine, is unlikely. One scheme consistent with available analytical data involves F or hydroxyl: $B(F,OH)Si_{-1}O_{-1}$, as proposed by Hinthorne and Ribbe (1974) and Deer et al. (1982, p. 400). B contents in olivine are equal to or exceed F contents (atomic basis, Table 9), allowing that some hydroxyl is probably also present to balance charge.

TABLE 7. Analyses of pargasite

	2 UM	5 UM	7 IGEM	8 UM
	Electron microprobe analyses—wt%			
SiO_2	38.85	42.59	44.92	42.27
TiO_2	0.54	0.02	0.03	0.04
Al_2O_3	19.29	15.52	13.58	14.96
Cr_2O_3	—	—	0.03	—
FeO	9.34	6.34	5.63	6.59
MnO	0.16	0.03	0.15	0.06
MgO	13.66	17.52	17.08	17.50
CaO	11.75	13.35	13.44	13.28
Na_2O	0.90	1.13	1.77	0.83
K_2O	3.55	2.00	1.93	2.10
Cl	0.39*	—	0.13	—
	Ion microprobe analyses—wt%			
Li_2O	0	0.005	—	0.003
B_2O_3	0.050	0.059	—	0.085
Rb_2O	0.005	0.006	—	—
SrO	0.02	0.03	—	0.036
BaO	0.04	0.01	—	0.01
F	0.45	1.94	—	0.98
	Calculated—wt%			
H_2O	1.73	1.24	2.07	1.61
Total	100.45	100.97	100.73	99.95
	Formulae normalized to 23 O atoms			
Si	5.698	5.942	6.394	6.102
Al	2.289	2.044	1.606	1.877
B	0.013	0.014	—	0.021
Total	8.0	8.0	8.0	8.0
Ti	0.060	0.002	0.003	0.004
Al	1.046	0.508	0.672	0.668
Cr	—	—	0.003	—
Fe	1.146	0.740	0.670	0.796
Mn	0.020	0.004	0.018	0.007
Mg	2.987	3.644	3.625	3.766
Li	0	0.003	—	0.002
Total	5.259	4.901	4.991	5.243
Ca	1.847	1.995	2.050	2.054
Na	0.256	0.306	0.489	0.232
K	0.664	0.356	0.350	0.387
Rb	0	0.001	—	—
Sr	0.002	0.002	—	0.003
Ba	0.002	0.001	—	0.001
Total	2.771	2.661	2.889	2.677
Total cat.	16.030	15.562	15.880	15.920
F	0.209	0.846	—	0.447
Cl	0.097	—	0.031	—
OH	1.694	1.154	1.969	1.553

Note: All Fe as FeO. OH + F + Cl assumed to equal 2. Totals corrected for O = F, O = Cl. UM and IGEM indicate the electron microprobe used.
* Measured at IGEM.

Plagioclase, clinozoisite, garnet, and thomsonite

Plagioclase in samples 8527 and 5152 is anorthite, An_{99} (Pertsev and Boronikhin, 1988; this study, Table 10).

Secondary clinozoisite derived from plagioclase is variable in Fe_2O_3 content (Table 10).

TABLE 8. Analyses of micas and chlorite

	1 Cln UM	— Cln* UM	2 Mrg IG	3 Phl(C)** UM	3 Phl(M)† UM	4 Phl UM	4 Chl UM	5 Phl UM	7 Phl UM
				Electron microprobe analyses—wt%					
SiO_2	16.82	16.47	30.86	38.88	39.03	38.53	27.55	40.26	40.68
TiO_2	0.02	0.02	0.01	0.53	0.44	0.65	0.02	0.01	0.05
Al_2O_3	43.25	44.79	51.04	16.78	16.61	16.39	23.95	14.60	14.34
Cr_2O_3	—	—	0.01	—	—	—	—	—	—
FeO	2.35	1.74	0.18	3.87	3.46	2.66	7.04	2.70	2.57
MnO	0.05	0	0.03	0.13	0.07	0	0.11	0	0.04
MgO	19.68	19.34	0.06	24.02	24.05	24.46	28.54	25.93	25.67
CaO	12.54	13.38	13.09	0	0.05	0.13	0.27	0.02	0.05
Na_2O	0.09	0.37	0.31	0.35	0.45	0.21	—	0.26	0.34
K_2O	0.01	0.01	0.10	10.68	10.60	10.48	—	10.42	10.54
				Ion microprobe analyses—wt%					
Li_2O	0.002	0.024	—	0.001	0.001	0.002	—	0.044	0.017
BeO	0.002	0	—	—	—	—	—	—	—
B_2O_3	0.009	0.01	—	0.02	0.01	0.007	—	0.02	0.008
Rb_2O	—	—	—	0.15	0.16	0.21	—	0.16	0.14
SrO	0.003	0.01	—	0.004	0.005	0.005	—	0.004	0.003
BaO	0.001	—	—	0.054	0.05	0.28	—	0.16	0.16
F	0.14	1.09	—	0.94	1.01	1.00	—	2.20	1.70
				Calculated—wt%					
H_2O	4.15	3.77	4.54	3.77	3.72	3.70	12.53	3.17	3.41
Total	99.06	100.56	100.23	99.78	99.29	98.29‡	100.01	99.03§	99.00§
				Formulae for 22 O atoms (micas), 28 O atoms (chlorite)					
Si	2.387	2.305	4.074	5.533	5.569	5.543	5.273	5.735	5.792
Al	5.610	5.692	3.926	2.462	2.429	2.455	2.727	2.261	2.206
Be	0.001	0	—	—	—	—	—	—	—
B	0.002	0.003	—	0.005	0.002	0.002	—	0.004	0.002
Total	8.000	8.000	8.000	8.000	8.0	8.0	8.0	8.0	8.0
Ti	0.002	0.002	0.001	0.057	0.047	0.070	0.003	0.001	0.005
Al	1.623	1.694	4.016	0.352	0.364	0.324	2.676	0.190	0.200
Cr	—	—	0.001	—	—	—	—	—	—
Fe	0.279	0.204	0.020	0.461	0.413	0.320	1.127	0.322	0.306
Mn	0.006	0	0.003	0.016	0.008	0	0.018	0	0.005
Mg	4.163	4.034	0.012	5.095	5.115	5.246	8.144	5.507	5.449
Li	0.001	0.013	—	0.001	0	0.001	—	0.025	0.010
Total	6.074	5.947	4.053	5.982	5.947	5.961	11.968	6.045	5.975
Ca	1.907	2.006	1.852	0	0.008	0.020	0.055	0.003	0.008
Na	0.025	0.100	0.079	0.097	0.124	0.059	—	0.072	0.094
K	0.002	0.002	0.017	1.939	1.929	1.923	—	1.894	1.915
Rb	—	—	—	0.014	0.015	0.019	—	0.015	0.013
Sr	0	0.001	—	0	0	0	—	0	0
Ba	0	—	—	0.003	0.003	0.016	—	0.009	0.009
Total	1.934	2.109	1.948	2.053	2.079	2.037	0.055	1.993	2.039
Total cat.	16.008	16.056	14.001	16.035	16.026	15.998	20.023	16.038	16.014
F	0.063	0.484	—	0.423	0.456	0.455	—	0.991	0.766
OH	3.937	3.516	4.0	3.577	3.544	3.545	16.000	3.009	3.234

Note: All Fe as FeO. Totals corrected for F = O. UM, IGEM, and IG indicate the electron microprobe used.
* Sample 136851, Melville Peninsula, Canada.
** Core.
† Margin.
‡ Cl present in amounts ≤0.2%.
§ Cl not detected.

Secondary garnet associated with chlorite in 516/372 (no. 4) is largely grossular-andradite, while that in sample 8527, an anorthite-clinopyroxene skarn containing scheelite and rare serendibite (Pertsev and Boronikhin, 1988), is nearly pure grossular (this study, Table 10). Si values below 6 per 24 O atoms and low analytical totals suggest some $4H^+ = Si^{4+}$ (hydrogrossular) substitution in these garnets.

Analysis of a fine-grained fibrous mineral occurring with clinozoisite, margarite, and blue tourmaline formed from anorthite breakdown in sample 5152 (no. 2) yields a stoichiometry close to $NaCa_2Al_5Si_5O_{20}$ (Table 10), the formula for thomsonite. However, more than $6H_2O$, the H_2O content per formula unit given for thomsonite, is needed to bring the analytical total to 100%.

Sinhalite and ludwigite

An analysis of sinhalite in an overgrowth around ludwigite in 485/858, 4V (no. 7) gave a reasonable analytical total assuming an ideal B content, $(Mg,Fe^{2+})AlBO_4$ (Table 11). However, analytical totals for ludwigite are high (103–104 wt%, Table 11). Ludwigite analyses were recalculated from $(Mg,Fe^{2+})_2(Fe^{3+},Al)BO_5$, the formula derived from single-crystal X-ray studies (Takeuchi et al., 1950; Norrestam et al., 1989), and we have no explanation for the high analytical totals. Ludwigite in sample 485/858, 2B

TABLE 9. Analyses of olivine and clinohumite

	5 Ol IGEM	5 Chu IGEM	6 Ol* UM	6 Chu UM	6 Chu UM	7 Ol* UM	7 Chu UM	8 Ol IGEM
				Electron microprobe analyses—wt%				
SiO_2	37.94	36.11	38.02	35.16	34.54	38.48	36.12	39.85
TiO_2	0	0.15	0.01	0.07	0.05	0.02	0.02	0.03
Al_2O_3	0	0.06	0.08	0.05	0.04	0.02	0.04	0
Cr_2O_3	0	0	—	—	—	—	—	—
FeO	14.45	8.97	11.64	7.98	7.88	11.33	10.36	12.97
MnO	0.29	0.21	0.27	0.33	0.16	0.27	0.25	0.30
MgO	46.75	50.01	48.72	51.77	51.79	49.07	49.34	45.63
CaO	0	0	0.05	0.07	0.05	0.04	0.02	0
Na_2O	0	0	—	—	—	—	—	0
				Ion microprobe analyses—wt%				
Li_2O	0.002	0.001	0.001	0.001	0.001	0.001	0.001	0.001
B_2O_3	1.14	0.37	1.11	1.10	1.13	1.35	0.86	1.11
F	0.60	3.46	0.33	4.26	1.88	0.55	1.05	0.39
				Calculated—wt%				
H_2O	—	1.11	—	0.76	1.86	—	2.27	—
Total	100.92	98.99	100.09	99.76	98.59	100.90	99.89	100.12
				Formulae per 4 oxygens (Ol), 17 oxygens (Chu)				
Si	0.943	3.941	0.940	3.794	3.761	0.942	3.911	0.986
B	0.049	0.070	0.047	0.204	0.212	0.057	0.161	0.047
Total	0.992	4.011	0.987	3.998	3.973	0.999	4.072	1.033
Ti	0	0.012	0	0.006	0.004	0	0.002	0.001
Al	0	0.008	0.002	0.006	0.005	0.001	0.005	0
Cr	0	0.000	—	—	—	—	—	—
Fe	0.301	0.819	0.241	0.720	0.718	0.232	0.938	0.268
Mn	0.006	0.019	0.006	0.030	0.015	0.006	0.023	0.006
Mg	1.734	8.138	1.796	8.327	8.406	1.791	7.963	1.680
Ca	0	0	0.001	0.008	0.006	0.001	0.002	0
Na	0	0	—	—	—	—	—	0
Li	0	0	0	0	0	0	0	0
Total	2.041	8.996	2.046	9.097	9.154	2.031	8.933	1.955
Total cat.	3.033	13.007	3.033	13.095	13.127	3.030	13.005	2.988
F	0.047	1.194	0.026	1.455	0.647	0.043	0.360	0.031
OH	—	0.806	—	0.545	1.353	—	1.640	—

Note: Fe as FeO. In clinohumite, assumed formula is $(Mg,Fe)_9(Si,B)_4O_{16}(OH,F)_2$. Totals corrected for F = O. UM and IGEM indicate the electron microprobe used.

* Ni sought but not detected.

(no. 5) is less magnesian than other Tayozhnoye ludwigite (20–29 wt% MgO, Lisitsyn et al., 1985; Pertsev and Boronikhin, 1986), whereas the range of Al_2O_3 contents in the newly analyzed samples (0.4–3.2 wt%, Table 11) overlaps the range reported by these authors, 0.49–2.7 wt% Al_2O_3.

Magnetite, spinel, and magnesite

Magnetite in the orthosilicate rocks approaches end-member Fe_3O_4 in composition with MgO the most abundant impurity (0.93–1.56 wt%, Table 12).

Spinel is a magnesian spinel-hercynite with variable amounts of Fe_2O_3 estimated by stoichiometry (Table 12). Spinel associated with tourmaline in three magnesian skarns contains less zinc (0.15–0.38 wt% ZnO) than spinel in the orthosilicate rocks (0.53–0.88 wt%).

A single carbonate grain adjacent to the analyzed tourmaline in 485/858, 2B is ferroan magnesite, $(Mg_{0.92}Fe_{0.07}Mn_{0.006}Ca_{0.005})CO_3$.

Element distribution

Assuming ideal F + OH contents, the ratio of F/OH increases Phl < Prg < Tur, Chu (except Chu in no. 7, Fig. 9). Phl < Prg is the reverse of experimentally determined

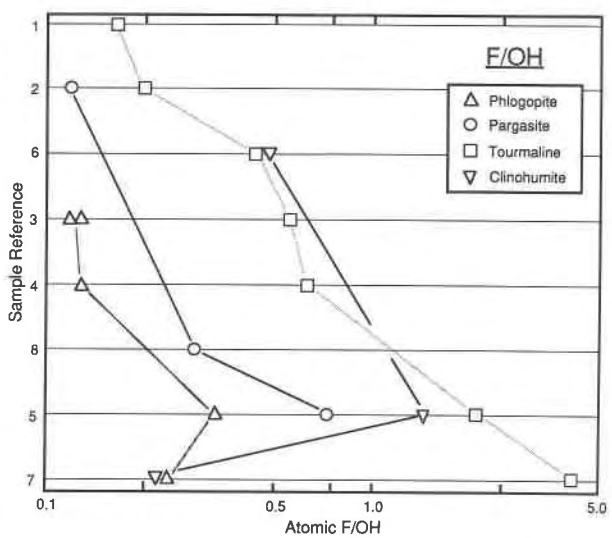

Fig. 9. Distribution of F and hydroxyl in Tayozhnoye ferromagnesian silicates plotted in a sequence of increasing ratio of F/OH of tourmaline on a semilogarithmic diagram (adapted from Albee, 1968). OH^- contents have been calculated from ideal formulations as follows, neglecting Cl in pargasite: OH + F = 4 (Phl), OH + F = 2 (Chu and Prg) and OH + F = 1 (Tur, from Deer et al., 1986). Sample references are taken from Table 2.

Table 10. Analyses of plagioclase, clinozoisite, thomsonite, and garnet

	2 Pl UM	2 Czo* IG	2 Tms UM	4 Grt UM	8527** Grt IGEM
Electron microprobe analyses—wt%					
SiO_2	43.08	37.76	35.65	35.95	38.74
TiO_2	—	0.03	0†	1.00	0.05
Al_2O_3	36.58	28.89	30.53	15.63	21.89
Fe_2O_3	—	6.78	—	8.13	0.50
FeO	0.16	—	0†	—	—
MnO	—	0.12	0†	0.14	0.45
MgO	—	0	0†	0.08	0.08
CaO	20.25	23.51	13.49	37.16	37.23
Na_2O	0.11	0.03	3.67	—	0
K_2O	0.01	0	0.01	—	0
Ion microprobe analyses—wt%					
Li_2O	0	—	0	—	—
B_2O_3	0.02	—	0.08	—	—
SrO	0.04	—	0.07	—	—
BaO	0	—	0†	—	—
Total	100.25	99.03	96.41‡	98.09	98.94
Formulae for eight O atoms (Pl), 12.5 O atoms (Czo), 20 O atoms (Tms), 12 O atoms (Grt)					
Si	1.994	2.956	4.967	2.871	2.957
B	0.001	—	0.019	—	—
Ti	—	0.002	0	0.060	0.003
Al	1.996	2.666	5.014	1.471	1.969
Fe	0.006	0.399	0	0.489	0.029
Mn	—	0.007	0	0.009	0.029
Mg	—	0	0	0.010	0.009
Ca	1.004	1.972	2.014	3.180	3.045
Na	0.010	0.005	0.992	—	0
K	0.001	0	0.002	—	0
Sr	0.001	—	0.006	—	—
Total	5.013	8.007	13.014	8.090	8.041

Note: All Fe as FeO in Pl, as Fe_2O_3 in Grt and Czo. UM, IGEM, and IG indicate the electron microprobe used.

* All Mn as Mn_2O_3. At two other spots, Fe_2O_3 = 5.96, 3.48 wt%. Total includes 1.91 wt% H_2O calculated from ideal formulation.

** Sample 8527, Pertsev and Boronikhin (1988).

† Not analyzed at UM, but found to be zero in an analysis done at IG. Be, Ba, and F were not detected in scan on ion microprobe.

‡ Includes 12.91 wt% H_2O calculated assuming $6H_2O$ per 20 O atoms.

Table 11. Analyses of sinhalite and ludwigite

	5 Lud* UM	7 Lud IGEM	7 Lud** UM	7 Snh** UM
		wt%		
SiO_2	—	0.25	—	—
TiO_2	0.15	0.37	0.30	—
Al_2O_3	0.41	3.15	1.63	40.39
Cr_2O_3	—	0.06	—	—
Fe_2O_3†	34.98	32.75	34.19	—
FeO	35.87	23.57	31.00	4.13
MnO	0.11	0.22	0.18	0
ZnO	—	0.04	—	—
MgO	16.16	25.33	20.36	29.19
Na_2O	—	0.22	—	—
K_2O	—	0.01	—	—
B_2O_3**	15.66	16.81	16.28	27.43
Total	103.35	102.78	103.93	101.14
Formulae for four cations, five O atoms (Lud); four O atoms (Snh)				
Si	—	0.009		
Ti	0.004	0.010	0.008	
Al	0.018	0.128	0.068	1.005
Cr	—	0.002	—	—
Fe^{3+}	0.974	0.849	0.916	—
Fe^{2+}	1.110	0.679	0.922	0.073
Mn	0.003	0.006	0.005	0
Zn	—	0.001	—	—
Mg	0.891	1.301	1.080	0.919
Na	—	0.015		
K	—	0		
B	1.000	1.000	1.000	1.000
Total	4.000	4.000	3.999	2.997

Note: CaO = 0. Sb and Sn sought but not detected in ludwigite (UM). UM and IGEM indicate the electron microprobe used.

* Fine prisms in olivine.

** Rounded ludwigite grain mantled in part by sinhalite and magnetite.

† Calculated from stoichiometry and assuming 1B per formula unit, except Snh, where all Fe assumed as FeO.

partitioning between phlogopite and pargasite (Westrich, 1981). K_d [= (F/OH)Tur/(F/OH)Phl] is 4.4–6.4 (17 in no. 7), substantially above the K_d values of 0.75–1.7 for tourmaline + biotite pairs in eight kornerupine-bearing samples (Grew et al., 1990b). Possibly the enhanced fractionation of F into tourmaline relative to biotite is caused by the substitution of Fe^{3+} for Mg in tourmaline on the *Y* site, which is bonded to O(1). The enhanced fractionation of F is suggested by the site occupancies in buergerite, in which the *Y* site is more than 60% occupied by Fe^{3+} and the O(1) site is occupied by F (Barton, 1969; Tippe and Hamilton, 1971). The contents of Fe^{3+} in the octahedral layer in associated biotite are probably less than that in the *Y* site of tourmaline; Guidotti and Dyar (1991) report that $^{[6]}Fe^{3+}$ = 10–13% and $^{[4]}Fe^{3+}$ = 8% of the total Fe in biotite associated with magnetite in pelitic rocks. The association of Fe^{3+} and F in tourmaline implies that "Fe-F avoidance" (e.g., Munoz, 1984, p. 472) applies only to Fe^{2+} and not to Fe^{3+}. An "Fe^{3+}-F attraction" deserves consideration as a factor in F-OH distribution.

In general, Na contents of the Tayozhnoye calc-silicate minerals are near the limit of detection; only tourmaline and pargasite incorporate significant amounts. Among serendibite localities overall, the ratio of Na/Ca increases (except where Na/Ca < 0.01), as follows: Pl, Cpx < Srd ≪ Scp, Prg, Tur (Fig. 10), a sequence consistent with the ratio of Na/Ca increasing Pl < Tur in pelitic rocks (Henry and Guidotti, 1985). The reversal in Tur-Prg relations with decreasing ratio of Na/Ca is caused by the modest decrease in the ratio of Na/Ca in pargasite as compared to the hundredfold decrease in the Na/Ca ratio in tourmaline, which parallels the decreases in the ratio of Na/Ca in serendibite and clinopyroxene in the more sodic samples. Contrasting site occupancies could explain these trends. In pargasite, Ca is restricted to the M(4) site, while Na vies with K on the A site and little, if any, Na is present on the M(4) site. On the other hand, Na substitutes for Ca on one site in tourmaline and clinopyroxene. In serendibite, Na substitutes for Ca on two sites, but the ratios of Ca/Na are similar at 3.4 and 4.6 on the two sites (P. K. Sen Gupta and G. H. Swihart, unpublished data on a Johnsburg serendibite; see also Sen Gupta et al., 1989).

Fe-Mg distribution is less regular than F-OH or Na-Ca distribution (Fig. 11), probably because Fe^{3+} and Fe^{2+} cannot be distinguished in electron microprobe analyses. Within the limitations imposed by ambiguities in the ratio of Fe^{2+}/Fe^{3+}, the sequence of increasing Mg/Fe^{2+} ratio is

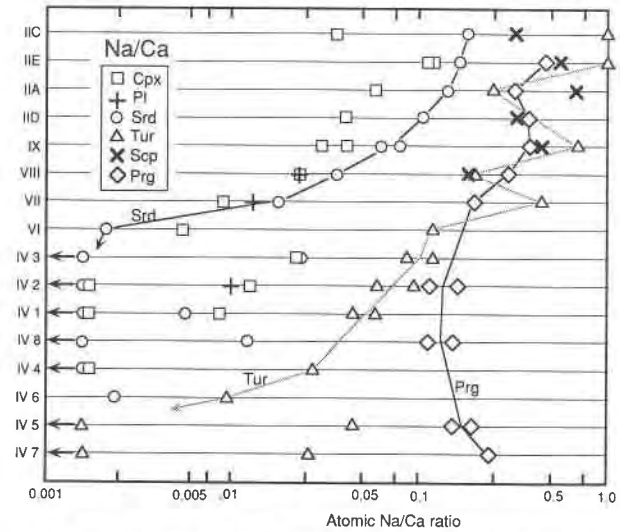

Fig. 10. Distribution of Na and Ca (atomic) is plotted in a semilogarithmic diagram (adapted from Albee, 1968). In sample reference (column at left), roman numerals refer to localities (Table 1), arabic numerals refer to Tayozhnoye sample numbers (Table 2), and letters refer to Johnsburg sample numbers as follows: A = Sl-4, B = 5231, C = Sl-3, D = 84-5, and E = 18964. In cases where more than one analysis is available, only the maximum and minimum ratios of Na/Ca are plotted. Arrows at left side indicate Na is below detection in these minerals. Na/Ca < 0.02 are approximate because of the difficulty of analyzing small quantities of Na_2O ($\leq$ 0.2 wt%). Localities II–VI (top half of diagram) are arranged according to decreasing ratio of Na/Ca in serendibite; locality IV (Tayozhnoye, bottom half), according to the ratio of Na/Ca in tourmaline.

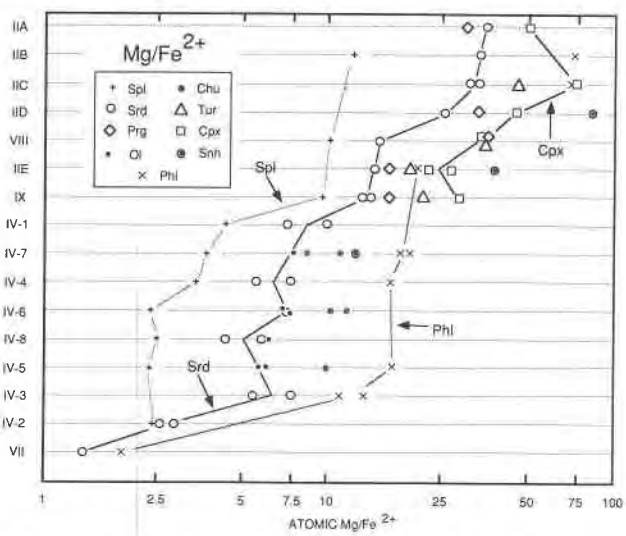

Fig. 11. Distribution of Mg and Fe (atomic) plotted in a sequence of decreasing ratio of Mg/Fe in serendibite or olivine on a semilogarithmic diagram (adapted from Albee, 1968). Numbering in column and plotting of maximum and minimum values follow the same system as in Figure 10. The only compositions plotted are those for which Mg/Fe^{2+} is inferred to differ little from the ratio of Mg/Fe_{tot} (Ol, Chu, Phl; all minerals with Mg/Fe > 9), or for which the ratio of Mg/Fe^{2+} can be estimated from stoichiometry (Srd, Spl with Mg/Fe < 9). For VII, 7 wt% B_2O_3 was assumed in calculating Mg/Fe^{2+} in serendibite.

TABLE 12. Analyses of spinel and magnetite

	1 Spl UM	2 Spl UM	4 Spl IGEM	5 Spl IGEM	6 Spl IGEM	6 Mag IGEM	7 Spl IGEM	8 Spl IGEM	8 Mag IGEM
					wt%				
SiO_2	—	—	0.00	0.00	0.16	0.34	0.11	0.00	0.13
TiO_2	0.04	0.06	0.03	0.03	0.03	0.13	0.00	0.00	0.12
Al_2O_3	64.31	62.74	68.64	66.22	66.52	0.66	65.26	65.74	0.45
Cr_2O_3	0.02	0.06	—	0.03	—	—	0.04	—	—
V_2O_3	0.00	0.03	—	—	—	—	—	—	—
Fe_2O_3	4.01	4.49	0.00	1.67	0.80	68.49	4.40	2.76	69.63
FeO	8.65	13.06	10.69	14.00	13.55	28.25	9.95	13.24	29.90
MnO	0.52	0.86	0.27	0.15	0.17	0.31	0.14	0.17	0.30
ZnO	0.27	0.15	0.38	0.58	0.53	0.19	0.88	0.78	—
MgO	21.20	18.12	20.68	18.42	18.57	1.56	20.82	18.77	0.93
CaO	—	—	0.00	0.00	0.00	0.04	0.00	0.00	0.00
Na_2O	—	—	0.00	0.00	—	—	0.11	0.00	0.00
K_2O	—	—	0.00	0.00	—	—	0.05	0.00	0.00
Total	99.02	99.57	100.69	101.10	100.33	99.97	101.76	101.46	101.46
				Formulae for four O atoms and three cations					
Ti	0.001	0.001	0.001	0.001	0.001	0.004	0.000	0.000	0.003
Al	1.922	1.909	2.002	1.966	1.984	0.030	1.917	1.948	0.020
Cr	0.000	0.001	—	0.001	—	—	0.001	—	—
Fe^{3+}	0.077	0.087	0.000	0.032	0.015	1.963	0.083	0.052	1.973
Total	2.000	1.999*	2.003	2.000	2.000	1.997	2.001	2.000	1.996
Fe^{2+}	0.183	0.282	0.221	0.295	0.287	0.900	0.207	0.278	0.942
Mn	0.011	0.019	0.006	0.003	0.004	0.010	0.003	0.004	0.010
Zn	0.005	0.003	0.007	0.011	0.010	0.005	0.016	0.014	—
Mg	0.801	0.697	0.763	0.692	0.700	0.089	0.773	0.703	0.052
Total	1.000	1.001	0.997	1.001	1.001	1.004	0.999	0.999	1.004
Total cat.	3.000	3.000	3.000	3.001	3.001	3.001	3.000	3.000	3.000

Note: Fe^{3+}/Fe^{2+} calculated from stoichiometry. UM and IGEM indicate the electron microprobe used.
* Includes 0.001 V^{3+}.

Spl < Srd, Ol ≤ Prg < Tur < Cpx, Phl and Ol < Chu. Thus the sequence for serendibite localities in general, including more Fe-rich assemblages, differs little from the sequence Grew et al. (1991) inferred for the Fe-poor Johnsburg assemblages.

Discussion

Features of serendibite parageneses

Serendibite mostly occurs in rocks containing substantial CaO, (Mg,Fe)O, Al_2O_3, and SiO_2, that is, aluminous calc-silicate assemblages such as magnesian skarns. Serendibite has not been found with quartz (see also Hutcheon et al., 1977), nor has it been found in carbonate rocks such as marble. Only two Ca-poor parageneses have been reported: the orthosilicate rocks from Tayozhnoye and a rock rich in potassium feldspar from Johnsburg.

In most cases, calc-silicate rocks containing serendibite from other localities are similar in mineralogy to the magnesian skarns from Tayozhnoye, and relationships among the minerals have many features in common. In particular, poikilitic tourmaline mantles around serendibite are characteristic of Tayozhnoye skarns, Johnsburg, Riverside, Handeni, and Russell. However, in contrast to coeval development of pargasite and serendibite in some Tayozhnoye skarns, pargasite formed later than serendibite in the Russell and Johnsburg skarns (Grew et al., 1990a, 1991), whereas tourmaline appears to have preceded serendibite in the Melville skarn (Hutcheon et al., 1977). The Ianapera rock differs from the other skarns in that serendibite apparently crystallized in an equilibrium assemblage Srd + Tur + Cpx + An + Hbl + Czo + Zo + Grs (Nicollet, 1988, 1990a). The last three minerals, as well as tourmaline, are clearly secondary in Tayozhnoye, Johnsburg, and Riverside skarns.

Serendibite-bearing skarns range from highly magnesian compositions (Johnsburg, Russell, Ihosy) to those intermediate in the ratio of Mg/Fe; the most Fe-rich serendibite has a $(Fe^{3+} + Fe^{2+})/Mg = 1.08$ (Ianapera, Madagascar, Nicollet, 1988, 1990a). The Johnsburg and Russell parageneses are distinctive in their relatively high ratios of Na/Ca and association with scapolite, thereby implying that serendibite is not restricted to Na-poor compositions, at least at intermediate pressures.

Minerals associated with serendibite have some distinctive compositional features, several of which are characteristic of high-temperature, silica-undersaturated magnesian (calc-silicate) skarns. Clinopyroxenes are moderately (2–5 wt% Al_2O_3) to extremely aluminous, reaching 18 wt% in the Ianapera sample (Nicollet, 1988). In the Johnsburg clinopyroxene samples, a significant part of the Al_2O_3 is incorporated as $NaAlSi_2O_6$ (Grew et al., 1991), whereas in the Tayozhnoye, Melville, and Ianapera clinopyroxene samples, it is incorporated largely as $Ca^{[6]}Al^{[4]}(AlSi)O_6$ and $Ca^{[6]}Fe^{3+\,[4]}(AlSi)O_6$ (Hutcheon et al., 1977; Nicollet, 1988; this study, Table 6). Hornblendes are pargasitic hornblende, pargasite, and in the Ianapera sample, the Na equivalent to magnesio-sadanagaite, for which Nicollet (1988) reports Si = 5.341 per formula unit. Plagioclase is anorthite (An_{98-99}, Pertsev and Boronikhin, 1988; Nicollet, 1988; this study, Table 7). With the exception of a few specimens from Johnsburg (Grew et al., 1991), sodic plagioclase is not found with serendibite. Sodian serendibite at Russell and Johnsburg occurs with scapolite [$X(Ca) = 0.59–0.75$, Grew et al., 1990a, 1991).

The Johnsburg and Tayozhnoye serendibite samples developed through metasomatism. By analogy, a metasomatic origin was inferred for Russell serendibite (Grew et al., 1990a) and such an origin appears to be plausible for the skarn rocks formed between two contrasting lithologies at the other localities listed in Table 1 (Deer et al., 1978). von Knorring (1967) and Bowden et al. (1969) described the Handeni assemblage as a skarn in marble, leaving open the possibility of a metasomatic origin, whereas Nicollet (1988, 1990a) suggested that the serendibite-bearing rocks at the two Madagascar localities are metarodingites into which B could have been introduced prior to, rather than during, metamorphism.

Petrogenetic grids for serendibite paragenesis

For comparison of different serendibite parageneses, we have developed two grids based on Schreinemakers diagrams in the model system CaO-MgO-Al_2O_3-SiO_2-B_2O_3-H_2O-CO_2 for the six phases serendibite, tourmaline (uvite), clinopyroxene, anorthite, calcite, and spinel. This simplification is justified in that other components, such as K_2O, TiO_2, MnO, and S, are minor constituents of the six phases. On the other hand, FeO, Fe_2O_3, and Na_2O are major constituents and their possible influence should be considered. H_2O, CO_2, and B_2O_3 are treated as perfectly mobile components, that is, the skarns behave as open systems with regard to these constituents, at least during formation of serendibite (see Korzhinskii, 1957). In addition, we have only considered parageneses associated with H_2O-rich fluids. This assumption appears to be reasonable for the early stages of metamorphism during which serendibite formed. It is justified for the later stages during which clintonite and grossular + chlorite formed, because clintonite and grossular + chlorite are characteristic of H_2O-rich fluids (Rice, 1983).

Disposition of the phases in the tetrahedron CaO-MgO-Al_2O_3-SiO_2 (inert components) or chemography is illustrated in Figure 12. The chemography is unambiguous except for the relative positions of tourmaline and serendibite, which appear to be nearly colinear with spinel and quartz. Had Fe_2O_3 contents been estimated for tourmaline and combined with Al_2O_3 (thereby deducting a corresponding amount of FeO added to MgO), as was done for serendibite and spinel, then tourmaline compositions would plot on the Al_2O_3 side of the serendibite-spinel and serendibite-quartz joins, as do the Fe-poor Johnsburg compositions (Grew et al., 1991). We have thus adopted the chemography of the Johnsburg compositions in constructing the Schreinemakers diagrams (insets in Figs. 13 and 14).

The invariant point involving six phases in an isothermal, isobaric $\mu(B_2O_3)$-$\mu(CO_2)$ diagram applicable for a

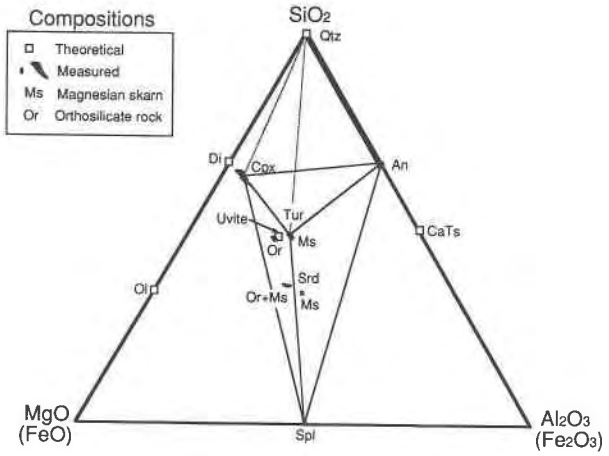

Fig. 12. Compositions of Tayozhnoye clinopyroxene (Cpx), uvite (Tur), serendibite (Srd), spinel (Spl), and anorthite (An) are plotted in terms of MgO, SiO_2, Al_2O_3, and CaO (projected from calcite). For Cpx and Tur, Fe is assumed to be FeO and combined with MgO. For Srd and Spl, the ratio of Fe^{3+}/Fe^{2+} has been estimated from stoichiometry, Fe_2O_3 is combined with Al_2O_3, and FeO is combined with MgO. CaTs is the calcium-Tschermak component, $Ca^{[6]}Al^{[4]}(AlSi)O_6$.

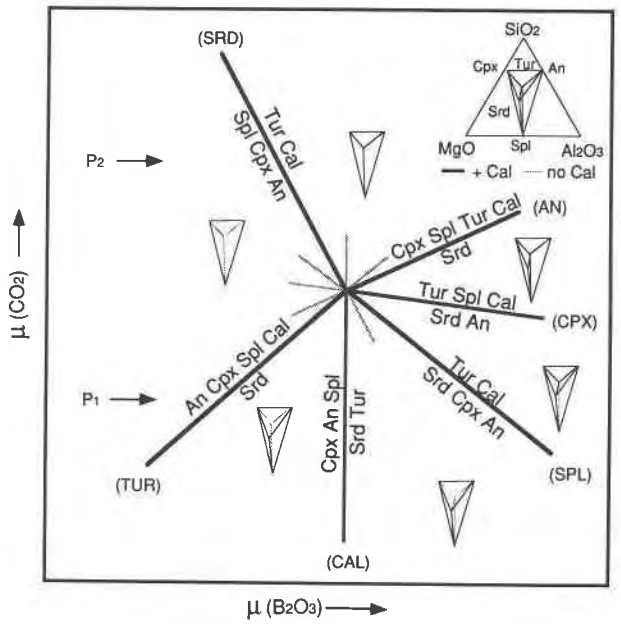

Fig. 13. Diagram of $\mu(CO_2)$-$\mu(B_2O_3)$ for invariant point involving six phases (Spl, Srd, Cpx, An, Tur, Cal) for the model system of four inert components (CaO, MgO, Al_2O_3, SiO_2) and three perfectly mobile components (CO_2, B_2O_3, H_2O). P_1 refers to low to intermediate pressures; P_2 refers to high pressures (see text). In compatibility diagrams, solid lines join phases coexisting with calcite; dashed lines join phases not coexisting with calcite.

specified H_2O activity (Fig. 13) should be applicable to the seven serendibite localities for which P-T conditions have been estimated, because estimated temperatures lie in a relatively narrow range (600–825 °C, Table 1). In addition, synthesis experiments in the CO_2-free system CaO-MgO-Al_2O_3-SiO_2-B_2O_3-H_2O have been carried out over a similar temperature interval, 600–800 °C, but with a wider range of pressures (1.8–20 kbar, G. Werding, N. N. Pertsev, and W. Schreyer, unpublished data). The experiments show that tourmaline coexists with serendibite over the range of pressures and temperatures studied. Figure 13 indicates that this assemblage would be stable at high $\mu(B_2O_3)$ and low $\mu(CO_2)$, that is, between the univariant reactions (An) and (Cal). These conditions apparently were not attained at the peak metamorphic temperatures at the localities listed in Table 1, except Ianapera and Melville Peninsula. At the other localities, there is little evidence for stable high-temperature Srd + Tur assemblages, although secondary Tur + Srd assemblages are common (see below). Consequently, $\mu(B_2O_3)$ probably did not exceed that for the invariant point, except at the Ianapera and Melville Peninsula localities.

At low $\mu(CO_2)$ in silica-undersaturated, spinel-bearing rocks, serendibite appears with increasing $\mu(B_2O_3)$, whereas at high $\mu(CO_2)$, tourmaline + calcite should appear. The relative abundance of Tur + Cal in the absence of spinel (e.g., Dunn et al., 1977; Deer et al., 1986; Povondra and Novak, 1986) compared to serendibite is caused by factors other than $\mu(CO_2)$, namely silica saturation, Na_2O, or both; Na_2O is preferentially fractionated into tourmaline and stabilizes it (Fig. 10).

The effect of Fe on tourmaline-serendibite relations is less obvious. Serendibite partitions Fe_{tot} relative to clinopyroxene and tourmaline, whereas spinel partitions Fe^{2+} relative to serendibite (Fig. 11). Most likely, any increase in the serendibite stability field caused by additional Fe^{2+} or Fe^{3+} is small compared to effects of other variables.

Figure 13 can also be used to deduce the effect of pressure on serendibite-tourmaline relations according to Korzhinskii's depth-facies principle, whereby $\mu(CO_2)$ increases with pressure [Pertsev, 1971, Fig. 36, applied this principle to the distribution of borates using the $\mu(CO_2)$-$\mu(B_2O_3)$ diagram]. At lower pressures, P_1, serendibite appears first as $\mu(B_2O_3)$ increases, whereas tourmaline requires much greater, apparently unattainable, $\mu(B_2O_3)$ in order to be stabilized with calcite. At the higher pressures, P_2, the sequence with increasing $\mu(B_2O_3)$ is reversed; tourmaline appears first and is stable with spinel and calcite. We are not aware of any reports of high-temperature prograde tourmaline + calcite + spinel assemblages. Tourmaline + spinel assemblages are not common (e.g., Pertsev, 1971); one example is the Tayozhnoye orthosilicate rock (Pertsev and Boronikhin, 1986; this study). However, carbonate is rare in these rocks and in the one case analyzed, turned out to be magnesite. Thus $\mu(CO_2)$, and corresponding pressures, may not exceed those of the invariant point. In summary, serendibite + anorthite + clinopyroxene assemblages, including those at Tayozhnoye, Ihosy, and Riverside, formed at relatively low $\mu(B_2O_3)$ and $\mu(CO_2)$ (corresponding to moderate to relatively low pressures) in the field between the univariant reactions (Tur) and (Cal).

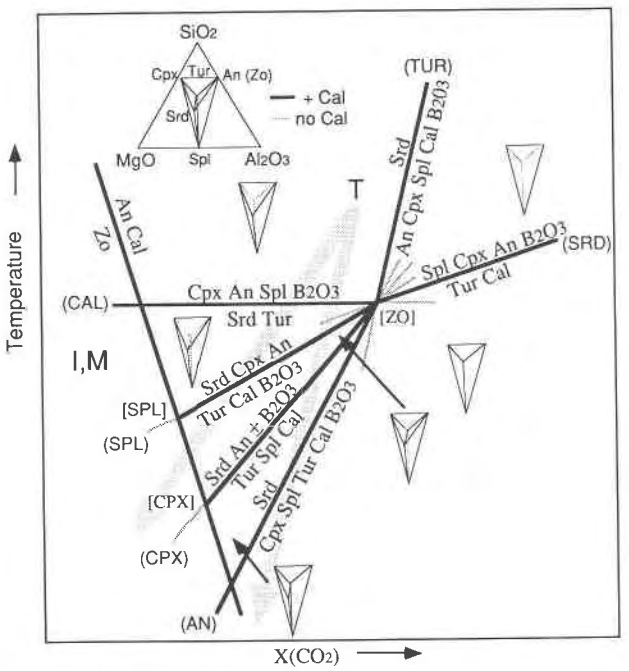

Fig. 14. Diagram of T-$X(CO_2)$ for the same invariant point as in Figure 13, here shown as [Zo]. The two invariant points involving zoisite, [Spl] and [Cpx], are not complete; reactions involving Zo with Srd or Tur are not shown. In compatibility diagrams, solid lines join phases coexisting with calcite; dashed lines join phases not coexisting with calcite. The inferred conditions for Tayozhnoye (T, including possible retrograde paths as broad arrows), Ianapera, Madagascar (I) and Melville Peninsula (M) are also shown.

A second perspective on serendibite petrogenesis is provided by a T-$X(CO_2)$ diagram of the same invariant point, which is labeled [Zo] in Figure 14. We suggest that this invariant point lies in the stability field of An + Cal. This assemblage is reported in the Ihosy, Madagascar assemblage (Nicollet, 1988), and calcite, in most cases secondary, occurs with anorthite and tourmaline in sample 5152 (Tayozhnoye). Assemblages with primary zoisite or clinozoisite (Ianapera, possibly Melville Peninsula) would have been stable with more H_2O-rich fluids. Rice (1983) calculated that the univariant reaction, Zo = An + Cal, decreases from $X(CO_2) = 0.3$ at 500 °C to 0.04 at 750 °C [P(fluid) = 5 kbar] and that clintonite and grossular + chlorite forms at T-$X(CO_2)$ conditions of the zoisite stability field. Thus Figure 14 can be used to infer possible retrograde paths (broad arrows) for Tayozhnoye. Serendibite crystallized at high temperatures in the field between the univariant reactions (Cal) and (Tur). Metamorphic evolution was one of decreasing temperature and $X(CO_2)$, so that in some cases, T-$X(CO_2)$ conditions attained those in the zoisite stability field. The paths first cut across the univariant reaction (Cal), stabilizing the assemblage Srd + Tur, as indicated by the serendibite relics in tourmaline (Fig. 2A). Then the paths cut the univariant reactions (Spl) and (Cpx), stabilizing Tur + Cal + Spl, an assemblage found in some poikilitic tourmaline mantles at Tayozhnoye and Johnsburg (Grew et al., 1991; this study, Figs. 2A, 2D). This assemblage, apparently unstable at high temperatures, appears to be stable at lower temperatures as a breakdown product of serendibite.

Conclusion

We now return to the question of what factors control the paragenesis of serendibite. This mineral is restricted to silica-undersaturated rocks formed at relatively high temperatures (600–825 °C) and low to intermediate pressures (<10 kbar). Low CO_2 activities are critical, as Nicollet (1988) noted. Introduction of H_2O-rich fluids at high temperatures would create favorable conditions for serendibite if B were available. At lower temperatures, CO_2 activities in aqueous fluids are sufficiently high to convert serendibite to its carbonated equivalent, tourmaline + spinel + calcite, which is commonly observed as a breakdown of serendibite. Metasomatic skarns, developed between contrasting rock types, provide a suitable environment for serendibite; at seven of the nine localities, serendibite has developed in this setting, and field data at the remaining two do not preclude a similar origin. Korzhinskii (1955) proposed a model whereby magnesian skarns, such as those in the Tayozhnoye deposit, formed while granitizing, dominantly aqueous fluids invade a contact between marble and quartzofeldspathic rock. At high temperatures, silica-undersaturated, spinel-bearing zones in the skarns would be suitable sites for serendibite formation, while tourmaline would form in more siliceous, spinel-free zones. This combination of silica-undersaturated skarns, metamorphosed at fairly high temperatures during influx of B-bearing aqueous fluids, is not commonly encountered in metamorphic terrains, and thus serendibite is a rare mineral.

Acknowledgments

We thank the following individuals and institutions for samples: the A.E. Fersman Mineralogical Museum of the U.S.S.R. Academy of Sciences, for three samples (including 5151 and 5158, latter is also no. 412M), M. Maleev, Sofia, for 5152, British Museum (Natural History) for BM 87050, National Museum of Natural History for 136851, T. Frisch for the Handeni specimen, Harvard Mineralogical Museum for 94852, and C. Nicollet for 261g and 320. We also thank A.A. Godovikov, P. Dunn, and C.A. Francis for information regarding the museum samples. In addition, we are grateful to N.V. Leskova for assistance with the electron microprobe at the Institute of Geology, Yakutsk; P.K. Sen Gupta and G.H. Swihart for providing unpublished crystallographic data on serendibite from samples 5151 and 5152; D.R. Veblen for unpublished information on olivine; and D.M. Morton for assistance in collecting at Riverside.

This paper has been much improved as a result of the critical reviews by D.M. Burt, J.V. Chernosky, P.C. Grew, C.V. Guidotti, and D.J. Henry.

This research was supported by U.S. National Science Foundation Grant DPP-8613241 to the University of Maine and by the interacademy exchange program between the U.S.S.R. and U.S.A. It was carried out within the framework of IGCP Project 235, "Metamorphism and Geodynamics."

References cited

Albee, A.L. (1968) Metamorphic zones in northern Vermont. In E-an Zen, W.S. White, J.B. Hadley, and J.B. Thompson, Jr., Eds., Studies of Appalachian geology: Northern and maritime, p. 329–341. Wiley, New York.

Barton, Randolf, Jr. (1969) Refinement of the crystal structure of buergerite and the absolute orientation of tourmalines. Acta Crystallographica, B25, 1524–1533.

Boronikhin, V.A., and Tsepin, A.I. (1980) A universal program for the real-time calculation of corrections and statistical processing of measurements during quantitative electron microprobe analysis. In Apparatus and methods of X-ray analysis, 23, p. 204–217. Leningrad (in Russian).

Bowden, P., von Knorring, Oleg, and Bartholemew, R.W. (1969). Sinhalite and serendibite from Tanzania. Mineralogical Magazine, 37, 145–146.

Coomaraswamy, A.K. (1902) The crystalline limestones of Ceylon. Quarterly Journal of the Geological Society of London, 58, 399–422.

Deer, W.A., Howie, R.A., and Zussman, J. (1978) In Rock-forming minerals, vol. 2A: Single-chain silicates (2nd edition), 668 p. Longman, London.

——— (1982) In Rock-forming minerals, vol. 1A: Orthosilicates (2nd edition), 919 p. Longman, London.

——— (1986) In Rock-forming minerals, vol. 1B: Disilicates and ring silicates (2nd edition), 629 p. Longman and Wiley, New York.

Dunn, P.J., Appleman, D., Nelen, J.A., and Norberg, J. (1977) Uvite, a new (old) common member of the tourmaline group and its implications for collectors. Mineralogical Record, 8, 100–108.

Grew, E.S. (1988) Kornerupine at the Sar-e-Sang, Afghanistan, whiteschist locality: Implications for tourmaline-kornerupine distribution in metamorphic rocks. American Mineralogist, 73, 345–357.

Grew, E.S., and Hinthorne, J.R. (1983) Boron in sillimanite. Science, 221, 547–549.

Grew, E.S., Yates, M.G., and deLorraine, W. (1990a) Serendibite from the northwest Adirondack Lowlands, in Russell, New York, USA. Mineralogical Magazine, 54, 135–137.

Grew, E.S., Chernosky, J.V., Werding, G., Abraham, K., Marquez, Nicholas, and Hinthorne, J.R. (1990b) Chemistry of kornerupine and associated minerals, a wet chemical, ion microprobe, and X-ray study emphasizing Li, Be, B and F contents. Journal of Petrology, 31, 1025–1070.

Grew, E.S., Yates, M.G., Swihart, G.H., Moore, P.B., and Marquez, Nicholas (1991) The paragenesis of serendibite at Johnsburg, New York, USA: An example of boron enrichment in the granulite facies. In L.L. Perchuk, Ed., Progress in metamorphic and magmatic petrology: A memorial volume in honor of D.S. Korzhinskiy, p. 247–285. Cambridge University Press, Cambridge, United Kingdom.

Grice, J.D., and Robinson, G.W. (1989) Feruvite, a new member of the tourmaline group, and its crystal structure. Canadian Mineralogist, 27, 199–203.

Guggenheim, Stephen (1984) The brittle micas. In Mineralogical Society of America Reviews in Mineralogy, 13, 61–104.

Guidotti, C.V., and Dyar, M.D. (1991) Ferric iron in metamorphic biotite and its petrologic and crystallochemical implications. American Mineralogist, 76, 161–175.

Henderson, J.R. (1983) Structure and metamorphism of the Aphebian Penrhyn Group and its Archean basement complex in the Lyon inlet area, Melville Peninsula, District of Franklin. Geological Survey of Canada Bulletin, 324, 50 p.

Henry, D.J., and Guidotti, C.V. (1985) Tourmaline as a petrogenetic indicator mineral: An example from the staurolite-grade metapelites of NW Maine. American Mineralogist, 70, 1–15.

Hinthorne, J.R., and Ribbe, P.H. (1974) Determination of boron in chondrodite by ion microprobe mass analysis. American Mineralogist, 59, 1123–1126.

Hutcheon, I., Gunter, A.E., and Lecheminant, A.N. (1977) Serendibite from Penrhyn Group Marble, Melville Peninsula, District of Franklin. Canadian Mineralogist, 15, 108–112.

Kohn, S.C., Henderson, C.M.B., and Mason, R.A. (1989) Element zoning trends in olivine phenocrysts from a supposed primary high-magnesian andesite: An electron- and ion-microprobe study. Contributions to Mineralogy and Petrology, 103, 242–252.

Korzhinskii, D.S. (1955) Outline of metasomatic processes. In Fundamental problems in the study of magmatogenic ore deposits (2nd edition), p. 335–453. U.S.S.R. Academy of Sciences, Moscow (in Russian).

——— (1957) The physico-chemical basis for the analysis of mineral parageneses, 184 p. U.S.S.R. Academy of Sciences, Moscow (in Russian; also 1959 translation, Consultants Bureau, New York).

Kulakovsky, A.L. (1985) Platinoids in rocks and ores of the Tayozhnoye skarn-magnetite deposit (Central Aldan). Doklady Akademii Nauk SSSR, 281, 129–133 (in Russian).

Kulakovsky, A.L., and Pertsev, N.N. (1986) Regeneration of magnesium orthosilicates and several aspects in the genesis of rich iron ores of the Tayozhnoye deposit (Central Aldan). Geologiya Rudnykh Mestorozhdeniy, 28 (2), 36–46 (in Russian).

——— (1987) Allochthonous carbonate rocks of the central Aldan Precambrian. Izvestiya Akademii Nauk SSSR, Seriya Geologicheskaya, 1987(1), 52–68 (in Russian).

Larsen, E.S., and Schaller, W.T. (1932) Serendibite from Warren County, New York, and its paragenesis. American Mineralogist, 17, 457–465.

Lisitsyn, A.Ye., Rudnev, V.V., Gaft, A.L., Dobrovol'skaya, N.V., Dara, O.M., and Tkacheva, T.V. (1985) New data on ludwigite and ascharite of the Tayozhnoye skarn-magnetite deposit (southern Yakutia). Zapiski Vsesoyuznogo Mineralogischeskogo Obshchestva, 1985(1), 62–73 (in Russian).

Marakushev, A.A. (1958) Petrology of the Tayozhnoye iron-ore deposit in the Archean of the Aldan Shield. Trudy Dal'nevostochnogo Filiala imeni V.L. Komarova Akademii Nauk SSSR, Seriya Geologicheskaya, vol. 5, 121 p. Magadan Press, Magadan (in Russian).

Matsubara, S., and Motoyoshi, Yoichi (1985) Potassium pargasite from Einstödingen, Lützow-Holm Bay, East Antarctica. Mineralogical Magazine, 49, 703–707.

Moore, P.B., and Araki, T. (1979) Kornerupine: A detailed crystal-chemical study. Neues Jahrbuch für Mineralogie Abhandlungen, 134, 317–336.

Munoz, J.L. (1984) F-OH and Cl-OH exchange in micas with applications to hydrothermal ore deposits. In Mineralogical Society of America Reviews in Mineralogy, 13, 469–493.

Nicollet, Christian (1988) Métabasites granulitiques, anorthosites et roches associées de la croûte inférieure. Exemples pris à Madagascar et dans le Massif Central français. Arguments en faveur d'un métamorphisme associé à l'extension lithosphèrique. Thèse d'Etat, Université Blaise Pascal, Clermont-Ferrand (in French).

——— (1990a) Crustal evolution of the granulites of Madagascar. In D. Vielzeuf and Ph. Vidal, Eds., Granulites and crustal evolution, p. 291–310. NATO ASI Series, Kluwer Academic Publishers, Dordrecht.

——— (1990b) Occurrences of grandidierite, serendibite, and tourmaline near Ihosy, southern Madagascar. Mineralogical Magazine, 54, 131–133.

Norrestam, R., Dahl, S., and Bovin, J.-O. (1989) The crystal structure of magnesium-aluminum ludwigite, $Mg_{2.11}Al_{0.31}Fe_{0.33}Ti_{0.05}Sb_{0.01}BO_5$, a combined single crystal X-ray and HREM study. Zeitschrift für Kristallographie 187, 201–211.

Pertsev, N.N. (1971) Parageneses of boron minerals in magnesian skarns, 192 p. Nauka, Moscow (in Russian).

Pertsev, N.N., and Boronikhin, V.A. (1986) Sinhalite, tourmaline, serendibite and ludwigite in magnetite ore of the Tayozhnoye deposit (Central Aldan). In A.A. Godovikov, Ed., New data on minerals, A.E. Fersman Mineralogical Museum of the USSR Academy of Sciences, 33, p. 143–147. Nauka, Moscow (in Russian).

——— (1988) Scheelite mineralization in skarn-magnetite deposits of the central Aldan. Mineralogicheskiy Zhurnal, 10(1), 94–97 (in Russian).

Pertsev, N.N., and Kulakovsky, A.L. (1987) Metasomatic quartzites, polymetamorphism and deformation in the Tayozhnoye iron-ore deposit (Central Aldan). In D.S. Korzhinskiy, L.L. Perchuk, and N.N. Pertsev, Eds., Regularities of metamagmatism, metasomatism and metamorphism, p. 101–118. Nauka, Moscow (in Russian).

——— (1988) Iron bearing complex of the central Aldan: Polymetamorphism and structural evolution, 237 p. Nauka, Moscow (in Russian).

Pertsev, N.N., and Nikitina, I.B. (1959) New data on serendibite. Zapiski Vsesoyuznogo Mineralogicheskogo Obshchestva, 88 (2), 169–172 (in Russian).

Povondra, P., and Novak, M. (1986) Tourmalines in metamorphosed carbonate rocks from western Moravia, Czechoslovakia. Neues Jahrbuch für Mineralogie Monatshefte, 1986(6), 273–282.

Prior, G.T., and Coomaraswamy, A.K. (1903) Serendibite, a new borosilicate from Ceylon. Mineralogical Magazine, 13, 224–227.

Rice, J.M. (1983) Metamorphism of rodingites: Part 1. Phase relations in a portion of the system CaO-MgO-Al_2O_3-SiO_2-CO_2-H_2O. American Journal of Science, 283-A, 121–150.

Richmond, G.M. (1939) Serendibite and associated minerals from the New City Quarry, Riverside, California. American Mineralogist, 24, 725–726.

Schaller, W.T., and Hildebrand, F.A. (1955) A second occurrence of the mineral sinhalite ($2MgO \cdot Al_2O_3 \cdot B_2O_3$). American Mineralogist, 40, 453–457.

Sen Gupta, P.K., Swihart, G.H., and Van Derveer, D.G. (1989) A restudy of the metal occupancies in serendibite. Geological Society of America Abstracts with Programs, 21 (6), A120.

Serdyuchenko, D.P. (1959) The origin of the Archean iron ores of South Yakutiya. Izvestiya Akademii Nauk SSSR, Seriya Geologicheskaya, 8, 34–49.

Shabynin, L.I. (1974) Ore deposits in magnesian skarn formations, 287 p. Nedra, Moscow (in Russian).

Shabynin, L.I., and Pertsev, N.N. (1956) Warwickite and serendibite from magnesian skarns of southern Yakutiya. Zapiski Vsesoyuznogo Mineralogicheskogo Obshchestva, 85 (4), 515–528 (in Russian).

Shimazaki, Hidehiko, Bunno, Michiaki, and Ozawa, Tohru (1984) Sadanagaite and magnesio-sadanagaite, new silica-poor members of calcic amphibole from Japan. American Mineralogist, 69, 465–471.

Steele, I.M., Hervig, R.L., Hutcheon, I.D., and Smith, J.V. (1981) Ion microprobe techniques and analyses of olivine and low-Ca pyroxene. American Mineralogist, 66, 526–546.

Takeuchi, Y., Watanabe, T., and Ito, T. (1950) The crystal structures of warwickite, ludwigite and pinakiolite. Acta Crystallographica, 3, 98–107.

Tippe, A., and Hamilton, W.C. (1971) A neutron-diffraction study of the ferric tourmaline, buergerite. American Mineralogist, 56, 101–113.

von Knorring, O. (1967) A skarn occurrence of sinhalite from Tanzania. Research Institute of African Geology of the University of Leeds 11th Annual Report (1965–1966), p. 40. Leeds, England.

Westrich, H.R. (1981) F-OH exchange equilibria between mica-amphibole mineral pairs. Contributions to Mineralogy and Petrology, 78, 318–323.

Wiechmann, M.J. (1988) Mineral assemblage zoning in the Crestmore (California) contact metasomatic aureole. Eos, 69, 514.

Yates, M.G., and Howd, F.H. (1988) Contact metamorphism of the Black Hawk Zn-Pb-Cu deposit, Hancock County, Maine. Maritime Sediments and Atlantic Geology, 24, 267–279.

Manuscript received February 1, 1990
Manuscript accepted February 11, 1991

Appendix 1. Mineral abbreviations

Anh = anhydrite, An = anorthite, Ap = apatite, Bt = biotite, Cal = calcite, Ccp = chalcopyrite, Chl = chlorite, Chu = clinohumite, Cpx = clinopyroxene, Czo = clinozoisite, Cln = clintonite, Crn = corundum, Di = diopside, Dol = dolomite, Ep = epidote, Fsp = feldspar, Grt = garnet, Gdd = grandidierite [$(Mg,Fe)Al_3BSiO_9$], Grs = grossular, Hbl = hornblende, Kfs = potassium feldspar, Lud = ludwigite [$(Mg,Fe^{2+})_2Fe^{3+}BO_5$], Mgs = magnesite, Mag = magnetite, Mrg = margarite, Ms = muscovite, Ol = olivine, Opx = orthopyroxene, Prg = pargasite, Phl = phlogopite, Pl = plagioclase, Po = pyrrhotite, Py = pyrite, Qtz = quartz, Spr = sapphirine, Scp = scapolite, Srd = serendibite, Srp = Serpentine, Snh = sinhalite [$(Mg,Fe)AlBO_4$], Spl = spinel, Tms = thomsonite, Ttn = titanite, Tr = tremolite, Tur = tourmaline, Zo = zoisite, Zrn = zircon.